



Two photon study of environmental effects on indole spectra  
by Aden Andrew Rehms

A thesis submitted in partial fulfillment of the requirements for the degree of Doctor of Philosophy in  
Chemistry

Montana State University

© Copyright by Aden Andrew Rehms (1990)

Abstract:

Polarized two-photon fluorescence excitation spectroscopy has been applied for the first time to the study of indole, the chromophore of the amino acid tryptophan. Investigations of three nine-membered ring systems, benzimidazole, benzimidazole cation, and indole have emphasized the utility of the experimental technique and revealed that the overlapping La and Lb states of indole have very different two-photon polarization ratios. Substituted indoles, with their varying La-Lb energy gaps, were studied in cyclohexane and n-butanol to explore the usefulness of the polarization ratio difference. The results of this study have directly confirmed the previously deduced La-Lb energy gaps in these compounds, the greater sensitivity of La to polar solvation, La-Lb level inversion, the role of La in producing broad red-shifted fluorescence, the existence of ground state complexes, and the importance of hydrogen bonding in the ground state complexes. The La Lb polarization ratio difference was also exploited to investigate the influence of charge on the La and Lb states. Experiments with tryptophan, 5-methoxytryptophan and yohimbine revealed the great sensitivity of the La state to a positive charge in the vicinity of the 5-ring of indole. The results with tryptophan also hint at a role of the Lb state in the dual exponential decay of tryptophan fluorescence. Two-photon spectra of all the aromatic amino acids and a comparison of the strength of their signals show tyrosine to be comparable to phenylalanine for two-photon excitation. Unlike the situation in one-photon spectroscopy, it may be possible to observe phenylalanine residues in proteins with two-photon spectroscopy. Finally, the first ever two-photon excitation spectrum of a small protein, melittin, shows that it is possible to observe a two-photon signal from a protein.

TWO PHOTON STUDY OF ENVIRONMENTAL  
EFFECTS ON INDOLE SPECTRA

by

Aden Andrew Rehms

A thesis submitted in partial fulfillment  
of the requirements for the degree

of

Doctor of Philosophy

in

Chemistry

MONTANA STATE UNIVERSITY  
Bozeman, Montana

February 1990

D378  
R2696

ii

APPROVAL

of a thesis submitted by

Aden Andrew Rehms

This thesis has been read by each member of the thesis committee and has been found to be satisfactory regarding content, English usage, format, citations, bibliographic style, and consistency, and is ready for submission to the College of Graduate Studies.

Feb 16, 1990

Date

Patrick R. Callis

Chairperson, Graduate Committee

Approved for the Major Department

January 13, 1990

Date

Edwin H. Abbott

Head, Major Department

Approved for the College of Graduate Studies

Feb 26, 1990

Date

Henry S. Parsons

Graduate Dean

## STATEMENT OF PERMISSION TO USE

In presenting this thesis in partial fulfillment of the requirements for a doctoral degree at Montana State University, I agree that the Library shall make it available to borrowers under rules of the Library. I further agree that copying of this thesis is allowable only for scholarly purposes, consistent with "fair use" as prescribed in the U.S. Copyright Law. Requests for extensive copying or reproduction of this thesis should be referred to University Microfilms International, 300 North Zeeb Road, Ann Arbor, Michigan 48106, to whom I have granted "the exclusive right to reproduce and distribute copies of the dissertation in and from microfilm and the right to reproduce and distribute by abstract in any format."

Signature

Robert A. Perkins

Date

1/8/90

## TABLE OF CONTENTS

	Page
INTRODUCTION . . . . .	1
EXPERIMENTAL . . . . .	4
Theory of Two-photon absorption . . . . .	4
Instrumentation and Procedures . . . . .	10
NINE-MEMBERED RING SYSTEMS: INDOLE AND BENZIMIDAZOLE . . . . .	17
Background . . . . .	17
Two-photon Spectra . . . . .	19
Discussion . . . . .	26
Indole . . . . .	26
Benzimidazole . . . . .	28
Benzimidazole Cation . . . . .	29
Summary . . . . .	30
SOLVENT AND SUBSTITUENT EFFECTS ON INDOLE . . . . .	31
Background . . . . .	31
Two-Photon Spectra . . . . .	35
Indoles in Cyclohexane . . . . .	35
5-methylindole (5MI) . . . . .	35
Indole . . . . .	35
1-methylindole (1MI) . . . . .	38
3-methylindole (3MI) . . . . .	38
2,3 dimethylindole (2,3MI) . . . . .	41
4-methoxyindole (4MI) . . . . .	43
5-methoxyindole (5MTI) . . . . .	43
6-methoxyindole (6MTI) . . . . .	46

TABLE OF CONTENTS -- Continued

	Page
7-methoxyindole (7MTI) . . . . .	48
Indoles in Butanol . . . . .	50
5-methylindole . . . . .	50
Indole . . . . .	50
1-methylindole . . . . .	55
3-methylindole . . . . .	55
2,3 dimethylindole . . . . .	55
4-methoxyindole . . . . .	55
5-methoxyindole . . . . .	64
6-methoxyindole . . . . .	64
7-methoxyindole . . . . .	64
Discussion . . . . .	64
Summary . . . . .	79
CHARGE EFFECTS . . . . .	81
Background . . . . .	81
Two-photon Spectra . . . . .	83
Discussion . . . . .	90
Summary . . . . .	97
AMINO ACIDS AND PROTEINS . . . . .	98
Background . . . . .	98
Two-photon Spectra . . . . .	99
Discussion . . . . .	105
Summary . . . . .	106

TABLE OF CONTENTS -- Continued

	Page
SUMMARY. . . . .	107
REFERENCES . . . . .	109

## LIST OF TABLES

Table	Page
1. INDO/s results for indoles studied. a) 10 x 20 singles only, Mataga-Nishimoto $\delta$ 's; b) 14 x 14 singles only Mataga-Nishimoto $\delta$ 's; c) 9 x 7 singles and doubles Ohno-Klopman $\delta$ 's . . . . .	27
2. Table of Results . . . . .	73

## LIST OF FIGURES

Figure	Page
1. Time-ordered Feynmann diagrams for a) A V coupling b) A A coupling and c) two consecutive A V couplings . . . . .	6
2. Laser apparatus utilized by the author to obtain the two-photon spectra in this study . .	12
3. Two-photon fluorescence excitation (solid line), one photon absorption (dashed line), and two-photon polarization (dotted line) spectra for indole dissolved in cyclohexane. (0.2M excitation, 0.05M polarization . . . . .	20
4. Two-photon fluorescence excitation (solid line), one photon absorption (dashed line), and two-photon polarization (dotted line) spectra for benzimidazole dissolved in isopropanol (0.2M) . . . . .	22
5. Two-photon fluorescence excitation (solid line), one photon absorption (dashed line), and two-photon polarization (dotted line) spectra for benzimidazole dissolved in methanol + H <sub>2</sub> SO <sub>4</sub> (0.2M) . . . . .	24
6. Relative two-photon absorptivities for indole, benzimidazole, benzimidazole cation, and toluene . . . . .	25
7. Indole ring numbering system . . . . .	31
8. Two-photon fluorescence excitation (solid line), one photon absorption (dashed line), and two-photon polarization (dotted line) spectra for 5-methylindole dissolved in cyclohexane (0.01M) . . . . .	36
9. Two-photon fluorescence excitation (solid line), one photon absorption (dashed line), and two-photon polarization (dotted line) spectra for indole dissolved in cyclohexane (0.01M) . . . . .	37

LIST OF FIGURES -- Continued

Figure	Page
10. Two-photon fluorescence excitation (solid line), one photon absorption (dashed line), and two-photon polarization (dotted line) spectra for 1-methylindole dissolved in cyclohexane (0.01M) . . . . .	39
11. Two-photon fluorescence excitation (solid line), one photon absorption (dashed line), and two-photon polarization (dotted line) spectra for 3-methylindole dissolved in cyclohexane (0.01M) . . . . .	40
12. Two-photon fluorescence excitation (solid line), one photon absorption (dashed line), and two-photon polarization (dotted line) spectra for 2,3-dimethylindole dissolved in cyclohexane (0.01M) . . . . .	42
13. Two-photon fluorescence excitation (solid line), one photon absorption (dashed line), and two-photon polarization (dotted line) spectra for 4-methoxyindole dissolved in cyclohexane (0.004M) . . . . .	44
14. Two-photon fluorescence excitation (solid line), one photon absorption (dashed line), and two-photon polarization (dotted line) spectra for 5-methoxyindole dissolved in cyclohexane (0.004M) . . . . .	45
15. Two-photon fluorescence excitation (solid line), one photon absorption (dashed line), and two-photon polarization (dotted line) spectra for 6-methoxyindole dissolved in cyclohexane (0.004M) . . . . .	47
16. Two-photon fluorescence excitation (solid line), one photon absorption (dashed line), and two-photon polarization (dotted line) spectra for 7-methoxyindole dissolved in cyclohexane (0.004M) . . . . .	49

LIST OF FIGURES -- Continued

Figure	Page
17. Two-photon fluorescence excitation (solid line), one photon absorption (dashed line), and two-photon polarization (dotted line) spectra for 5-methylindole dissolved in butanol (0.01M) . . . . .	51
18. Two-photon polarization spectra of 5-methylindole in cyclohexane (solid line) and in butanol (dotted line) (0.01M) . . . . .	52
19. One-photon absorption and fluorescence spectra of 5-methylindole in cyclohexane (solid lines) and in butanol (dotted lines) ( $\sim 10^{-5}M$ ) . . . . .	52
20. Two-photon fluorescence excitation (solid line), one photon absorption (dashed line), and two-photon polarization (dotted line) spectra for indole dissolved in butanol (0.01M) . . . . .	53
21. Two-photon polarization spectra of indole in cyclohexane (solid lines) and in butanol (dotted line) (0.01M) . . . . .	54
22. One-photon absorption and fluorescence spectra of indole in cyclohexane (solid lines) and in butanol (dotted line) (0.01M) . . . . .	54
23. Two-photon fluorescence excitation (solid line), one photon absorption (dashed line), and two-photon polarization (dotted line) spectra for 1-methylindole dissolved in butanol (0.01M) . . . . .	56
24. Two-photon polarization spectra of 1-methylindole in cyclohexane (solid line) and in butanol (dotted line) (0.01M) . . . . .	57
25. One-photon absorption and fluorescence spectra of 1-methylindole in cyclohexane (solid lines) and in butanol (dotted lines) ( $\sim 10^{-5}M$ ) . . . . .	57

LIST OF FIGURES -- Continued

Figure	Page
26. Two-photon fluorescence excitation (solid line), one photon absorption (dashed line), and two-photon polarization (dotted line) spectra for 3-methylindole dissolved in butanol (0.01M) . . . . .	58
27. Two-photon polarization spectra of 3-methylindole in cyclohexane (solid line) and in butanol (dotted line) (0.01M) . . . . .	59
28. One-photon absorption and fluorescence spectra of 3-methylindole in cyclohexane (solid lines) and in butanol (dotted lines) ( $\sim 10^{-5}M$ ) . . . . .	59
29. Two-photon fluorescence excitation (solid line), one photon absorption (dashed line), and two-photon polarization (dotted line) spectra for 2,3-dimethylindole dissolved in butanol (0.01M) . . . . .	60
30. Two-photon polarization spectra of 2,3-dimethylindole in cyclohexane (solid line) and in butanol (dotted line) (0.01M) . . . . .	61
31. One-photon absorption and fluorescence spectra of 2,3-dimethylindole in cyclohexane (solid lines) and in butanol (dotted lines) ( $\sim 10^{-5}M$ ) . . . . .	61
32. Two-photon fluorescence excitation (solid line), one photon absorption (dashed line), and two-photon polarization (dotted line) spectra for 4-methoxyindole dissolved in butanol (0.004M) . . . . .	62
33. Two-photon polarization spectra of 4-methoxyindole in cyclohexane (solid line) and in butanol (dotted line) (0.004M) . . . . .	63
34. One-photon absorption and fluorescence spectra of 4-methoxyindole in cyclohexane (solid lines) and in butanol (dotted lines) ( $\sim 10^{-5}M$ ) . . . . .	63

LIST OF FIGURES -- Continued

Figure	Page
35. Two-photon fluorescence excitation (solid line), one photon absorption (dashed line), and two-photon polarization (dotted line) spectra for 5-methoxyindole dissolved in butanol (0.004M) . . . . .	65
36. Two-photon polarization spectra of 5-methoxyindole in cyclohexane (solid line) and in butanol (dotted line) (0.004M) . . . . .	66
37. One-photon absorption and fluorescence spectra of 5-methoxyindole in cyclohexane (solid lines) and in butanol (dotted lines) (~10 <sup>-5</sup> M) . . . . .	66
38. Two-photon fluorescence excitation (solid line), one photon absorption (dashed line), and two-photon polarization (dotted line) spectra for 6-methoxyindole dissolved in butanol (0.004M) . . . . .	67
39. Two-photon polarization spectra of 6-methoxyindole in cyclohexane (solid line) and in butanol (dotted line) (0.004M) . . . . .	68
40. One-photon absorption and fluorescence spectra of 6-methoxyindole in cyclohexane (solid lines) and in butanol (dotted lines) (~10 <sup>-5</sup> M) . . . . .	68
41. Two-photon fluorescence excitation (solid line), one photon absorption (dashed line), and two-photon polarization (dotted line) spectra for 7-methoxyindole dissolved in butanol (0.004M) . . . . .	69
42. Two-photon polarization spectra of 7-methoxyindole in cyclohexane (solid line) and in butanol (dotted line) (0.004M) . . . . .	70
43. One-photon absorption and fluorescence spectra of 7-methoxyindole in cyclohexane (solid lines) and in butanol (dotted lines) (~10 <sup>-5</sup> M) . . . . .	70

LIST OF FIGURES -- Continued

Figure	Page
44. Comparison of the effect of polar solvation on the polarization spectra of indole and 1-methylindole. Indole in cyclohexane (dashed line) and in butanol (dash-dotted line). 1-methylindole in cyclohexane (solid line) and in butanol (dotted line) . . . . .	75
45. Comparison of the effect of polar solvation on the fluorescence spectra of indole (solid lines) and 1-methylindole (dotted lines). In each case the broad fluorescence is that seen in polar solvents . . . . .	78
46. Permanent dipole moments for the ground ( $\mu_g$ ), Lb ( $\mu_{Lb}$ ), and La ( $\mu_{La}$ ) states of indole . . . . .	82
47. Structure of Yohimbine . . . . .	82
48. Two-photon fluorescence excitation (solid line), one photon absorption (dashed line), and two-photon polarization (dotted line) spectra of Yohimbine dissolved in isopropanol at high pH ( $5 \times 10^{-3}M$ ) . . . . .	84
49. Two-photon fluorescence excitation (solid line), one photon absorption (dashed line), and two-photon polarization (dotted line) spectra of Yohimbine dissolved in isopropanol at low pH ( $5 \times 10^{-3}M$ ) . . . . .	85
50. Two-photon fluorescence excitation (solid line), one photon absorption (dashed line), and two-photon polarization (dotted line) spectra of 5-methoxytryptophan in pH 11 phosphate buffer (0.01M) . . . . .	87
51. Two-photon fluorescence excitation (solid line), one photon absorption (dashed line), and two-photon polarization (dotted line) spectra of 5-methoxytryptophan in pH 7 phosphate buffer (0.01M) . . . . .	88

LIST OF FIGURES -- Continued

Figure	Page
52. Two-photon fluorescence excitation (solid line), one photon absorption (dashed line), and two-photon polarization (dotted line) spectra of 5-methoxytryptophan in pH 2 phosphate buffer (0.01M) . . . . .	89
53. Two-photon fluorescence excitation (solid line), one photon absorption (dashed line), and two-photon polarization (dotted line) spectra of tryptophan in pH 11 phosphate buffer (0.01M) . . . . .	91
54. Two-photon fluorescence excitation (solid line), one photon absorption (dashed line), and two-photon polarization (dotted line) spectra of tryptophan in pH 7 phosphate buffer (0.01M) . . . . .	92
55. Two-photon fluorescence excitation (solid line), one photon absorption (dashed line), and two-photon polarization (dotted line) spectra of tryptophan in pH 2 phosphate buffer (0.01M) . . . . .	93
56. Comparison of the polarization spectra of tryptophan at pH 2 (solid line), pH 7 (dotted line) and pH 11 (dashed line) . . . . .	94
57. Two-photon fluorescence excitation (solid line), one photon absorption (dashed line), and two-photon polarization (dotted line) spectra of phenylalanine in pH7 buffer (0.01M) . . . . .	100
58. Two-photon fluorescence excitation (solid line), one photon absorption (dashed line), and two-photon polarization (dotted line) spectra of tyrosinamide in pH 7 buffer . . . . .	101
59. Two-photon fluorescence excitation (solid line), one photon absorption (dashed line), and two-photon polarization (dotted line) spectra of tryptophan in pH 7 buffer . . . . .	102

LIST OF FIGURES -- Continued

Figure	Page
60. Relative signal from typtophan (solid line), tyrosinamide (dashed line), and phenylalanine (dotted line) measured at their respective fluorecence maxima . . . . .	103
61. Two-photon fluorecence excitation (solid line) and two-photon polarization spectra for the monomeric (dotted line) and tetrameric (dashed line) forms . . . . .	104

## ABSTRACT

Polarized two-photon fluorescence excitation spectroscopy has been applied for the first time to the study of indole, the chromophore of the amino acid tryptophan. Investigations of three nine-membered ring systems, benzimidazole, benzimidazole cation, and indole have emphasized the utility of the experimental technique and revealed that the overlapping  $L_a$  and  $L_b$  states of indole have very different two-photon polarization ratios. Substituted indoles, with their varying  $L_a$ - $L_b$  energy gaps, were studied in cyclohexane and n-butanol to explore the usefulness of the polarization ratio difference. The results of this study have directly confirmed the previously deduced  $L_a$ - $L_b$  energy gaps in these compounds, the greater sensitivity of  $L_a$  to polar solvation,  $L_a$ - $L_b$  level inversion, the role of  $L_a$  in producing broad red-shifted fluorescence, the existence of ground state complexes, and the importance of hydrogen bonding in the ground state complexes. The  $L_a$ - $L_b$  polarization ratio difference was also exploited to investigate the influence of charge on the  $L_a$  and  $L_b$  states. Experiments with tryptophan, 5-methoxytryptophan and yohimbine revealed the great sensitivity of the  $L_a$  state to a positive charge in the vicinity of the 5-ring of indole. The results with tryptophan also hint at a role of the  $L_b$  state in the dual exponential decay of tryptophan fluorescence. Two-photon spectra of all the aromatic amino acids and a comparison of the strength of their signals show tyrosine to be comparable to phenylalanine for two-photon excitation. Unlike the situation in one-photon spectroscopy, it may be possible to observe phenylalanine residues in proteins with two-photon spectroscopy. Finally, the first ever two-photon excitation spectrum of a small protein, melittin, shows that it is possible to observe a two-photon signal from a protein.

## INTRODUCTION

The near ultraviolet absorption and fluorescence of proteins can be ascribed to the aromatic amino acids phenylalanine, tyrosine, and tryptophan (1). Absorption and emission of light by these amino acids have been exploited to study protein structure and dynamics (2,3,4,). The most useful of these is tryptophan, whose indole chromophore is highly sensitive to local solvation and structural environment. The lowest energy UV absorption band of indole consists of two nearly degenerate electronic transitions designated  $L_a$  and  $L_b$  (5). One photon studies have indicated that solvent(6,7,8,9,10), substitution (7,8,9), and charge (11) can differentially shift the  $L_a$  and  $L_b$  states and lead to large changes in the fluorescence spectra of indoles. This occurs without great alterations to their absorption spectra (12,13,14,15).

Perhaps the most notable characteristic of indole photophysics is the large stokes shift of the fluorescence in polar media. Red shifts of the fluorescence relative to that seen in hydrocarbon solvents occur for additions of polar solvent insufficient to alter the bulk dielectric properties of the solvent. Accompanying the red shift is a loss of structure in the fluorescence. It appears that polar solvents interact with indoles in a specific manner (12,13,14). Solvents also seem to have more general effects

on the fluorescence (15,16,17,18,19). The hypotheses advanced to explain how the solvent causes the large red shift of indole fluorescence are based upon solvent shift studies of absorption and fluorescence peaks.

Unfortunately, the broad nature of the transitions and complications due to dual absorption and emission from the  $L_a$  and  $L_b$  states make such studies subject to errors. What has been needed to resolve some of these questions is a way of separating the contribution of each state to these processes. Polarized fluorescence excitation has been used to resolve the band shapes of  $L_a$  and  $L_b$  in polar solvents (20,21) but has failed in hydrocarbon solvents where minute amounts of polar impurities complex with indoles at the low temperatures necessary to perform the experiments (22). Substituent perturbation (9,23) and derivative spectroscopy (24) have also been tried with largely unsatisfactory results.

Polarized two-photon fluorescence excitation offers a direct method of observing the  $L_a$  and  $L_b$  states separately in absorption. This technique involves the essentially simultaneous absorption of visible photons to reach excited states of ultraviolet energies. The simultaneous nature of the absorption makes it possible to observe a polarization dependence from non-rigid samples. It was discovered as part of this thesis work (25) that the  $L_a$  and  $L_b$  states of indole are characterized by very different two-photon

polarization ratios. This enabled the author to directly observe regions of  $L_a$  and  $L_b$  absorption.

The aim of this thesis was to utilize this powerful technique to learn more about the relative response of  $L_a$  and  $L_b$  to solvent, substitution, and charge. Indole and various of its methyl and methoxy derivatives were examined in hydrocarbon and alcohol solvents. Models for charge interactions, which included the amino acid tryptophan itself, were also examined. These two-photon experiments represent the first time this technique has been used to look at indoles and were designed to answer specific questions about the validity of conclusions drawn from the indirect one photon methods used by others. The results for these models systems combined with two-photon spectra of all the aromatic amino acids and a small protein, melittin, serve to pave the way for two-photon spectroscopy of proteins. INDO/S calculations have been compared to the experimental results to test their predictions so that they might also prove useful for interpretation of indole and protein spectra.

**EXPERIMENTAL**Theory of Two-photon absorption

The simultaneous absorption of two non-resonant photons by matter was first postulated to occur by Maria Goeppert-Mayer in 1931 (26). Observation of this phenomenon at optical frequencies had to await the advent of the laser (27) because of the inherently low transition probabilities associated with two-photon processes. Once practical, this new spectroscopy offered many unique possibilities and was quickly utilized to investigate a large number of compounds (28,29). Theoretical advances (30-40) of the period allowed experiments to be designed and gave a deeper insight into the regularities emerging in two-photon spectra of aromatic molecules.

Second order time-dependent perturbation theory predicts that molecules can absorb two photons through two types of interaction with the radiation. The relativistically invariant form of the Hamiltonian for a system in the presence of an electromagnetic field is given by (41)

$$H = \frac{1}{2m} \left( p - \frac{e}{c} A \right)^2 + [V(r) + e\phi]$$

where  $A$  is the vector potential of the radiation field given by

$$A(r,t) = A_0 \cos(\omega t - k \cdot r)$$

$\phi$  is the scalar potential associated with the electromagnetic field, and  $V(r)$  is an effective potential for a given electron due to the nuclei and other electrons in the system. Writing all the terms of equation 1 in detail, the Hamiltonian is

$$H = \frac{1}{2m} (-\hbar^2 \nabla^2 + i\hbar \frac{e}{c} \mathbf{A} \cdot \nabla + \frac{e^2}{c^2} |\mathbf{A}|^2) + V(r) + e\phi$$

If the coulomb gauge is chosen, it provides that  $\nabla \cdot \mathbf{A} = 0$  and  $\phi = 0$ . The equation above becomes

$$H = \frac{1}{2m} (-\hbar^2 \nabla^2 + 2i\hbar \frac{e}{c} \mathbf{A} \cdot \nabla + \frac{e^2}{c^2} |\mathbf{A}|^2) + V(r)$$

Rewriting this as

$$H = H^0 + H' = \left[ -\frac{\hbar^2}{2m} \nabla^2 + V(r) \right] + \left[ \frac{ie\hbar}{mc} \mathbf{A} \cdot \nabla + \frac{e^2}{2mc^2} |\mathbf{A}|^2 \right]$$

it is clear that the perturbation is

$$H' = \frac{ie\hbar}{mc} \mathbf{A} \cdot \nabla + \frac{e^2}{2mc^2} |\mathbf{A}|^2$$

These two terms describe the coupling with the electromagnetic field that lead to changes in the state function of the system. In Figure 1 are the time ordered Feynmann (42) diagrams which correspond to the couplings described by the  $\mathbf{A} \cdot \nabla$  and  $\mathbf{A} \cdot \mathbf{A}$  terms. The straight upward arrows represent a molecule moving through time and space in state  $\psi^0$  and the wiggly arrows are photons which may interact with the molecule and leave the molecule in a state  $\psi_{\pm}$ . Since the  $\mathbf{A} \cdot \mathbf{A}$  term involves 2 photons it makes no contribution to ordinary one photon processes. The calculations of McClain and Harris (31), Honig et al.

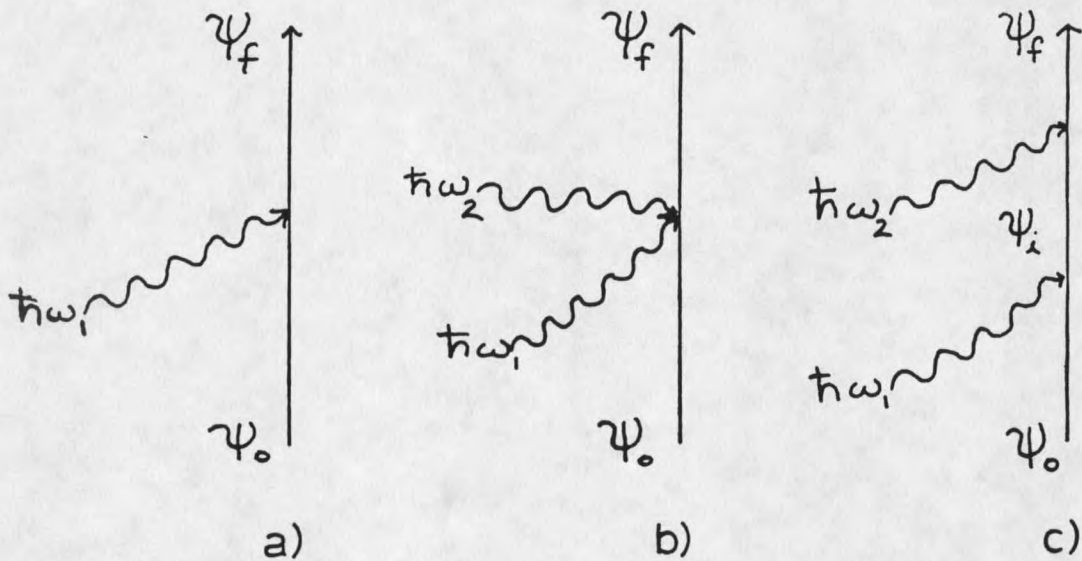


Figure 1: Time-ordered Feynmann diagrams for a)  $A \cdot \nabla$  coupling b)  $A \cdot A$  coupling and c) two consecutive  $A \cdot \nabla$  couplings.

(32,33), and Guccione and Van Kranendonk (43) have indicated that even for two photon absorption, the  $A \cdot A$  term gives little contribution. The Hamiltonian can now be taken as

$$H^0 = H^0 + H' = \left[ \frac{-\hbar^2}{2m} \nabla^2 + V(r) \right] + \frac{ie\hbar}{mc} A \cdot \nabla$$

With the appropriate Hamiltonian it is possible to proceed with a time-dependent perturbation treatment to arrive at the perturbed wavefunction in second order.

$$\psi_0^{(2)}(r,t) = \psi_0^{(1)}(r,t) + \frac{q^2 \nabla^2 \omega^2}{\hbar^2} \frac{\Sigma}{f} S_{\sigma \neq \mu} \mu_r^{\sigma}(r) \left( \frac{1 - \exp[-i(\omega_{\neq \sigma} - 2\omega)]}{\omega_{\neq \sigma} - 2\omega} \right)$$

Like one-photon processes, the transition rate for the two-photon process is proportional to the square of the coefficient of the final state  $\mu_r^{\sigma}$ . It is (31)

$$W_{g \leftarrow f}^{(2)} = 128\pi^3 \alpha^2 \omega^2 F^2 |S_{g \leftarrow f}|^2 g_m(2\omega)$$

This equation demonstrates the quadratic dependence of the transition rate on the photon flux (F) which distinguishes two-photon from one-photon processes. Dividing out the flux gives a purely molecular quantity,  $\delta_{g \leftarrow f}$ , the two-photon absorptivity, given by (31)

$$\delta_{g \leftarrow f} = 128\pi^3 \alpha^2 |S_{g \leftarrow f}|^2 g_m(2\omega)$$

In both cases above  $S_{g \leftarrow f}$  (assuming 2 identical photons) is (31)

$$S_{g \leftarrow f} = \frac{\sum (e \cdot \langle f | r | k \rangle) (\langle k | r | g \rangle \cdot e)}{k \omega_{k \leftarrow g} - \omega}$$

$S_{g \leftarrow f}$ , the two-photon tensor, demonstrates the complementary nature of one and two-photon processes. The dipole moment operator appears twice in  $S_{g \leftarrow f}$  and both transitions  $k \leftarrow g$  and  $f \leftarrow k$  must be parity allowed (i.e. one-photon allowed) for the two-photon transition to be allowed. For gerade ground states this corresponds to successive  $u \leftarrow g$  and  $g \leftarrow u$  transitions for an overall  $g \leftarrow g$  parity selection rule. The Feynmann diagram, which corresponds to the two successive  $A \cdot V$  couplings suggested by the two-photon tensor, is also shown in Figure 1.

The states  $|k\rangle$  over which the tensor is summed are termed intermediate states and should include the initial and final states (35,39,40). Inclusion of the ground and final states is especially important in the description of polar molecules, where there are states characterized by

large changes in permanent dipole moment (39). This can be seen by looking only at the two terms in the sum over intermediate states which correspond to the ground and final states as intermediate states. The two terms are:

$$S = \frac{\langle f|r|g\rangle\langle g|r|g\rangle}{\omega_{gg}-\omega} + \frac{\langle f|r|f\rangle\langle f|r|g\rangle}{\omega_{fg}-\omega}$$

If the matrix elements of the dipole operator are denoted in the form  $R_{xy}$  this can be written as

$$S_{\text{partial}} = \frac{R_{fg} R_{gg}}{\omega_{gg}-\omega} + \frac{R_{ff} R_{fg}}{\omega_{fg}-\omega}$$

Recognizing that  $\omega_{gg} = 0$  and  $\omega_{fg} = 2\omega$  for identical photons

$$S_{\text{partial}} = \frac{R_{fg} R_{gg}}{-\omega} + \frac{R_{ff} R_{fg}}{\omega}$$

which leads to

$$S_{\text{partial}} = \frac{R_{fg}}{\omega} (R_{ff} - R_{gg})$$

$R_{fg}$  is simply the matrix element of a one-photon (dipole induced) transition from the ground state to the final state and  $(R_{ff} - R_{gg})$  is the difference in the permanent dipole moment of final and ground states. Thus, for the ground and final states to be important as intermediate states, the transition must be one-photon allowed and there must be a considerable change in permanent dipole moment between the ground and final states. Such an addition to  $S_{gf}$  is not important for centrosymmetric molecules, but is for polar molecules like the indoles studied in this thesis. If the transition dipole and the change in dipole moment are collinear, an additional contribution to  $\delta_{gf}$  proportional to

the oscillator strength of the transition  $f \leftarrow g$  and the square of the change in dipole moment given in debyes is introduced. The contribution of dipole terms for equally polarized photons of the same energy in the case where  $R_{fg}$  is parallel to  $R_{ff} - R_{gg}$  is in gm given by (39)

$$\delta_{\uparrow\uparrow} = 1.043 \frac{f(\Delta\mu)^2}{\Delta E}$$

where  $f$  is the oscillator strength of  $f \leftarrow g$ ,  $\Delta\mu$  is the change in dipole moment (in debyes), and  $\Delta E$  is the excitation energy in eV. Excitation energies of 5eV associated with strong one-photon transitions ( $f=1$ ) and changes of dipole moment on the order of 2 debyes will produce extra two-photon absorptivity contributions as strong as a moderately intense two-photon transition (i.e., 1 Göppert-Mayer,  $1 \text{ gm} = 1 \times 10^{-50} \text{ cm}^2 \text{ sec}/\text{photon molecule}$ ).

The 3 x 3 cartesian tensorial nature of the two-photon process leads to a polarization dependence of  $\delta$  upon the light which survives averaging over all molecular orientations. This is not true for one-photon processes where the cross-section has no polarization dependence. The quantities which survive the orientation averaging are denoted  $\epsilon_f$ ,  $\epsilon_g$ , and  $\epsilon_h$  are defined as: (28)

$$\delta_f = S_{\alpha\alpha} S_{\beta\beta}^* = \sum_1^3 |\text{diagonal elements}|^2$$

$$\delta_g = S_{\alpha\beta} S_{\alpha\beta} = \sum_1^3 |\text{each element}|^2$$

$$\delta_h = S_{\alpha\beta} S_{\beta\alpha} = \sum_1^3 |\text{hermitian products}|$$

Identical photons from the same laser beam make  $\delta_g = \delta_h$ . Information about the elements of the tensor can still be obtained from the relation for the absorptivity of circularly versus linearly polarized light. This quantity,  $\Omega$ , the two-photon polarization ratio, is defined as (37)

$$\Omega = \frac{\delta_{\text{cir}}}{\delta_{\text{lin}}} = \frac{\delta_x + 3\delta_y}{\delta_x + 2\delta_y}$$

Upper and lower limits on the value of  $\Omega$  are exhibited by tensors with the following patterns of elements.

$$\begin{pmatrix} 0 & 1 & 1 \\ 1 & 0 & 1 \\ 1 & 1 & 0 \end{pmatrix}$$

$$\Omega = 3/2$$

$$\begin{pmatrix} 1 & 0 & 0 \\ 0 & 1 & 0 \\ 0 & 0 & 1 \end{pmatrix}$$

$$\Omega = 0$$

The value of  $\Omega$  will in general be different for every transition. Molecules which are symmetric will exhibit characteristic tensor patterns for each symmetry species. In order to assign a polarization ratio to a given state for molecules which lack symmetry it is necessary to rely upon approximate molecular orbital calculations such as CNDO/S and INDO/S (35,36,38).

### Instrumentation and Procedures

The two-photon fluorescence excitation spectra recorded in this study were obtained using the apparatus drawn schematically in Figure 2. The spectra of benzimidazole,

benzimidazole cation, and indole in cyclohexane were taken with an NRG 0.5 MW (peak) nitrogen pump laser and an NRG single stage scanning dye laser as the light source. Early work on the methylindoles (44) also utilized this laser system. Subsequent spectra of the methylindoles and the spectra of all other molecules were obtained using a Lumonics HD 300 dye laser (8ns, <13mJ/pulse) pumped by the 2nd or 3rd Harmonic of a JK HY200 Nd:YAG laser. A Gallilean telescope expanded and collimated the dye laser beam. It was then routed through a shutter to the glan polarizer which polarized it vertically. A double fresnel rhombahedron on a rotating mount served to rotate the plane of polarization 45° before the beam passed through a stationary fresnel rhombahedron. Linearly and circularly polarized light utilized for measuring  $\Omega$  were produced here. The shutter and the double rhomb were both rotated by stepping motors under computer control. The beam was either left unfocused or focused slightly from 8 mm in diameter to 4-6 mm in diameter, depending upon the dye being utilized and the sample characteristics. In all cases the peak power density at the sample was below  $1.25 \times 10^{10} \text{ Wm}^{-2}$ . The signal from the sample was also checked for quadratic behavior by attenuating the beam with crossed polarizers. If the quadratic condition was met, a reduction of the laser energy by 50% led to a two-photon excited fluorescence signal of

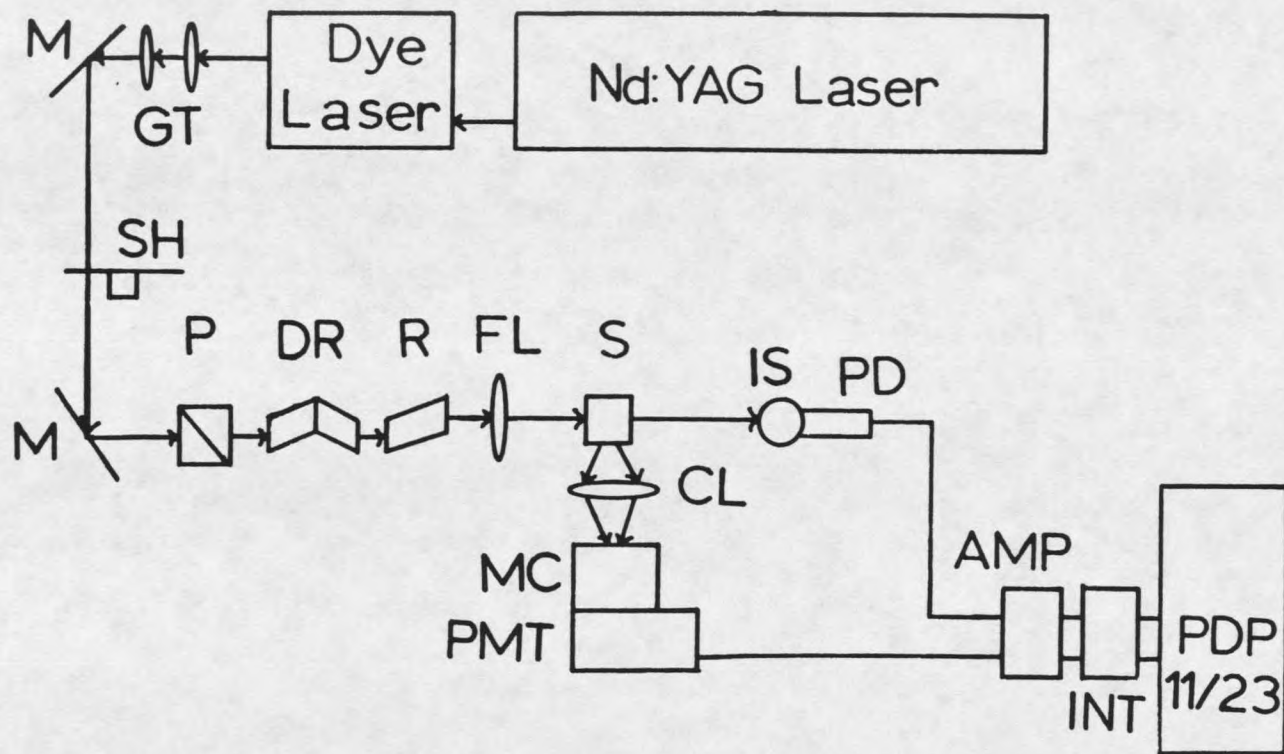


Figure 2: Laser apparatus utilized by the author to obtain the two-photon spectra in this study. GT (gallilean telescope), M (mirror), SH (shutter), P (glan polarizer), DR (double fresnel rhomb), R (fresnel rhomb), FL (focussing lens), S (sample), IS (integrating sphere), PD (photodiode), CL (cylindrical lens), MC (monochromator), PMT (photomultiplier tube), AMP (amplifier), INT (integrator).

25% of the original. These checks were performed at both ends of the dye ranges, the maxima of the dye gain curves, and at peaks due to molecular transitions. Defocusing was performed if necessary. The fluorescence of the sample was collected at right angles by an f3.0 quartz cylindrical lens, which focused it through 2 UV-pass filters (Schott UG-11) and onto the slit of an f/3.3 holographic grating monochromator (Instruments SA, 50 nm bandpass, 16 nm for early work where polarizer was rotated). No slits were used because slight changes in beam height due to the rotation of the double rhomb moved the beam off of the slit, giving a low reading for the circular signal. The laser beam was passed through the sample and into an integrating sphere where a quantum counting solution and a photodiode generated a signal proportional to the average photon flux. Below 600 nm Rhodamine (3g/l) was used as the quantum counter and above 600 nm, Nile Blue (1g/l). The fluorescence signal and the reference signal were amplified and integrated (200  $\mu$ s) using printed circuit boards purchased from Evans Associates. Integrated signals were stored and processed by a PDP 11/23 computer which also controls the stepping motors and the laser scan control unit. In a typical experiment the signals from the sample fluorescence and the laser reference detectors were averaged for 400 shots. The average of the sample signal was then divided by the square of the reference signal to obtain the normalized two-photon

signal. This was done at each wavelength using linearly polarized light to measure the two-photon fluorescence excitation spectrum. Determinations of the two-photon polarization ratio ( $\Omega$ ) were made at each wavelength using circularly polarized light for excitation and dividing the resulting two-photon signal by that just obtained for linearly polarized excitation.

Nine organic dyes and mixtures thereof covering a wavelength range of 440 nm to 650 nm were utilized in the dye laser to obtain the data segments. At least 5 nm of overlap was maintained between dye segments and they were joined to create the two-photon spectra. A more exact method of joining these segments to create a complete two-photon excitation spectrum has been developed recently by Jones and Callis (45). Within the range of 600 nm to 650 nm, this SHG technique was used as published. It involves second harmonic generation (SHG) from a powder sample of potassium di-hydrogen phosphate (KDP) to obtain a reference signal proportional to the instantaneous photon flux squared. The signal is used to compensate for changes in the temporal and spatial profiles of the laser beam to which the one photon reference is insensitive. In an attempt to extend the technique to shorter wavelengths, suspensions of urea crystals (75-150  $\mu\text{m}$ ) in decalin were tried. A quantum counting solution of 1g/l skatole in n-butanol was also added to remove the strong wavelength dependence below

600 nm of the UV pass filters used to separate the second harmonic from the fundamental. These efforts were successful in extending the technique with reasonable confidence to 530 nm where absorption by the decalin and possible scattering due to the mismatch of the refractive indices of decalin and urea caused the corrected two-photon signal to increase. Where reliable SHG data was obtained the procedure was utilized. All segments, corrected or not, were joined at the middle of the overlap and truncated so as to maintain the shape indicated by the midsection of each segment.

All solutes and solvents were of the highest quality available and used as received. Solutions were checked with 1-photon fluorescence excitation (Spex Fluorolog) and revealed no interfering fluorescent impurities. All solutions were approximately 0.01M except as indicated. Absorption spectra of dilute ( $10^{-5}$  M) solutions were obtained with a Cary 14 spectrophotometer. Fluorescence spectra were taken with the Spex Fluorolog.

Relative two-photon absorptivities ( $\delta$ ) for the benzimidazoles, toluene, and indole were determined by measuring the relative fluorescence signal excited by one and two-photon absorption. A 150 W Xenon arc lamp and a 0.5M grating monochromator were used for UV excitation. The detection geometry for both one and two-photon excitation

was kept constant. The relative two-photon absorptivity was then calculated from the relation

$$S_A^{(2)}/S_B^{(2)} = \epsilon_A C_A \phi_A(\lambda_A) / \epsilon_B C_B \phi_B(\lambda_B)$$

where  $S^{(2)}$  is the photon flux normalized two-photon signal for sample A,  $C_A$  its concentration, and  $\phi_A(\lambda_A)$  its differential fluorescence quantum yield.  $\phi$  represents the probability an absorbed photon will be emitted between wavelength  $\lambda$  and  $\lambda+d\lambda$ . The assumption of  $S_A^{(2)} = G\phi_A(\lambda_A)$  where  $G$  is the combined instrumental response function allowed calculation of  $\delta_s$ . Underlying the whole procedure is the assumption that the quantum yield per excitation is the same for one and two-photon excitation.

Molecular orbital calculations of one and two-photon properties were performed using a spectroscopically calibrated INDO/S program originally obtained from Dr. Michael Zerner, University of Florida(46), coupled to programs for calculating transition densities and two-photon properties.(47,48) Mataga-Nishimoto and Ohno-Klopman electron repulsion integrals were used for singly and doubly excited configuration calculations respectively.

**NINE-MEMBERED RING SYSTEMS: INDOLE AND BENZIMIDAZOLE**Background

Nine-membered heterocyclic aromatic ring systems are important in nature. They are found as the side chain of the amino acid tryptophan and are the basis for the nucleic acids adenine and guanine. These systems are non-alternate and lack symmetry, making it necessary to rely mostly upon semi-empirical molecular orbital calculations for theoretical insight. (48,49,50) The two lowest singlet  $\pi^* \leftarrow \pi$  states for indole have been assigned (1)  $L_B$  ( $S_1$ ) and  $L_a$  ( $S_2$ ) where the operational difference between the two states is that  $L_B$  is structured while  $L_a$  is broad and unstructured. This assignment appears to have followed the perimeter model classification scheme introduced by Platt. (5) While the  $L_a$  and  $L_B$  labels are meaningless for the odd-atom perimeter, a similarity exists between the transition density pattern (48) of the nine-ring states and the  $L_a$  and  $L_B$  states of benzene. Evleth (49) has also noted a similarity in the configuration wave functions.

The parent molecule for the nine-membered 10 pi electron series is the cyclononatetraenide anion. In this molecule the  $L_a$  and  $L_B$  states are degenerate. Callis (48) has discussed how cross-linking to form the 5-6 fused ring system of the indenyl anion ( $C_9H_7^{1-}$ ) removes this degeneracy. The  $L_a$  state appears to be mixed with the  $B_a$  state due to a

large  $L_a$ - $B_a$  transition density between the atoms that are cross-linked. The result is that the  $L_a$  state is greatly shifted to the red of the  $L_b$  state. Introduction of the nitrogen to form indole results in a cancellation of the effect of the cross-link and shifts the  $L_a$  state to the blue so that the two states are nearly degenerate again but with the  $L_b$  state now lowest. Introduction of another nitrogen at the 3 position to make benzimidole further shifts the  $L_a$  to the blue, separating them again. The inductive effect of the nitrogen has been discussed by Feitelson(50) as arising mainly from differences in the electrical charge distribution between the ground and excited states at the site of the nitrogen atom and he stressed the importance of including the interaction between the ground and excited states in the description of heteroatomic indene derivatives. He reasoned that since the inductive effect shifted the  $L_a$  and  $L_b$  states in different directions to leave  $L_b$  lowest for indole, electron donating groups at the 1 or 3 positions would lessen the inductive effect and lead to less of a blue shift for the  $L_a$  state. Indeed, the broad  $L_a$  state has been shown to move closer to the  $L_b$  state for tryptophan (3-substitution) (6) The importance of the charge density of the nitrogen can also be seen in Evleth's(49) work where moderate changes in the nitrogen parameters, leading to less of an inductive effect actually caused the  $L_a$  state to again become lowest for indole.

Since two-photon spectroscopy offers information complementary to that obtained with conventional one-photon spectroscopies, two-photon fluorescence excitation spectra of indole, benzimidazole, and benzimidazole cation were obtained. These experimental results have been used to judge the validity of INDO/S calculations. In order to further test the theory, measurements of relative two-photon absorptivities were made.

### Two-photon Spectra

Shown in Figure 3 are the two-photon fluorescence excitation for linearly polarized light (solid line), one-photon absorption (dashed lines), and two-photon polarization ratio (dotted lines) spectra for indole (0.2M). As is done throughout this thesis, the one-photon absorption is shifted from its one-photon wavelengths to correspond to wavelengths for two-photon absorption of the same total energy. The 0-0 of the absorption spectrum is also normalized to follow the 0-0 peak of the two-photon spectrum. The polarization spectrum shown is that obtained for a 0.05M solution.  $\Omega$  is seen to be near the theoretical maximum for the 0-0  $L_b$ . It then drops steeply, presumably due to the onset of  $L_a$  absorption, and levels off at  $\sim 0.7$ . The slight drop of the polarization ratio on the red edge is

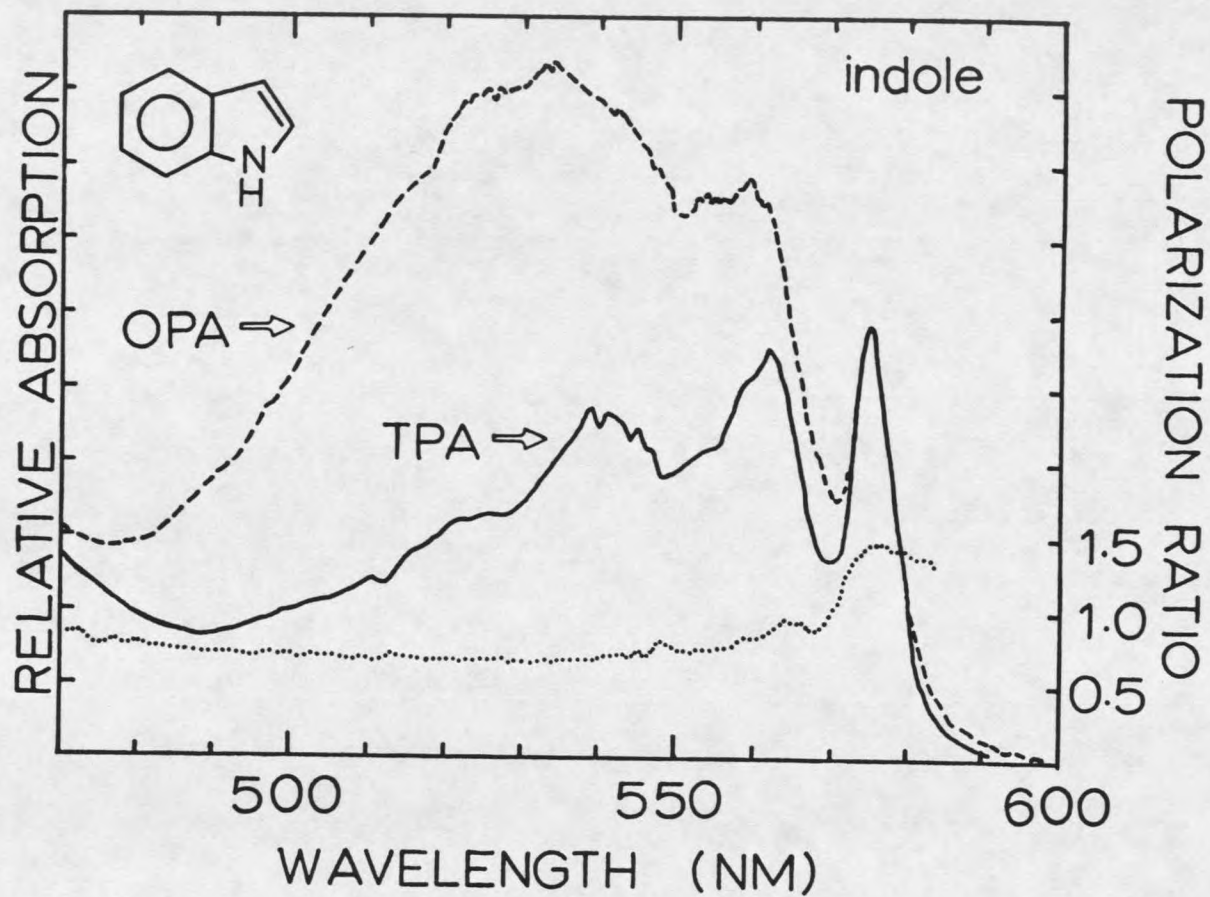


Figure 3: Two-photon fluorescence excitation (solid line), one photon absorption (dashed line), and two-photon polarization (dotted line) spectra for indole dissolved in cyclohexane. (0.2M excitation, 0.05M polarization)

concentration dependent and may be due to intermolecular hydrogen bonding. NMR experiments of concentrated solutions support this contention.(51) Little change is seen once the concentration is below 0.10 M. The two-photon excitation spectrum shows that the broad  $L_a$  band is less pronounced in two-photon than in one-photon excitation, but still outweighs the  $L_b$  band by a factor of four.

At this point some comment should be made about the apparent profile of the two-photon excitation spectra. The spectra presented in this section were obtained using the  $N_2$  laser described previously. Later two-photon spectra utilizing the Nd:YAG system appear to follow the one-photon spectra more closely and then deviate above them at higher energies. The effect seems to be due to the laser and not the detection system. This uncertainty precludes detailed discussion of relative  $L_a$  and  $L_b$  strengths in these molecules, but the wealth of information contained in the two-photon polarization ratio still makes this a very powerful technique.

In Figure 4 are shown spectra for benzimidazole (0.2 M Isopropanol). The two-photon excitation spectrum follows the one-photon absorption through both the 0-0 and the 0-1 of the  $L_b$  band. At approximately  $0+1550\text{cm}^{-1}$  there appears a peak which does not appear at all in the one-photon spectrum. With a spacing similar to that of the 0-0 and 0-1 a second peak, also missing in the one-photon absorption,

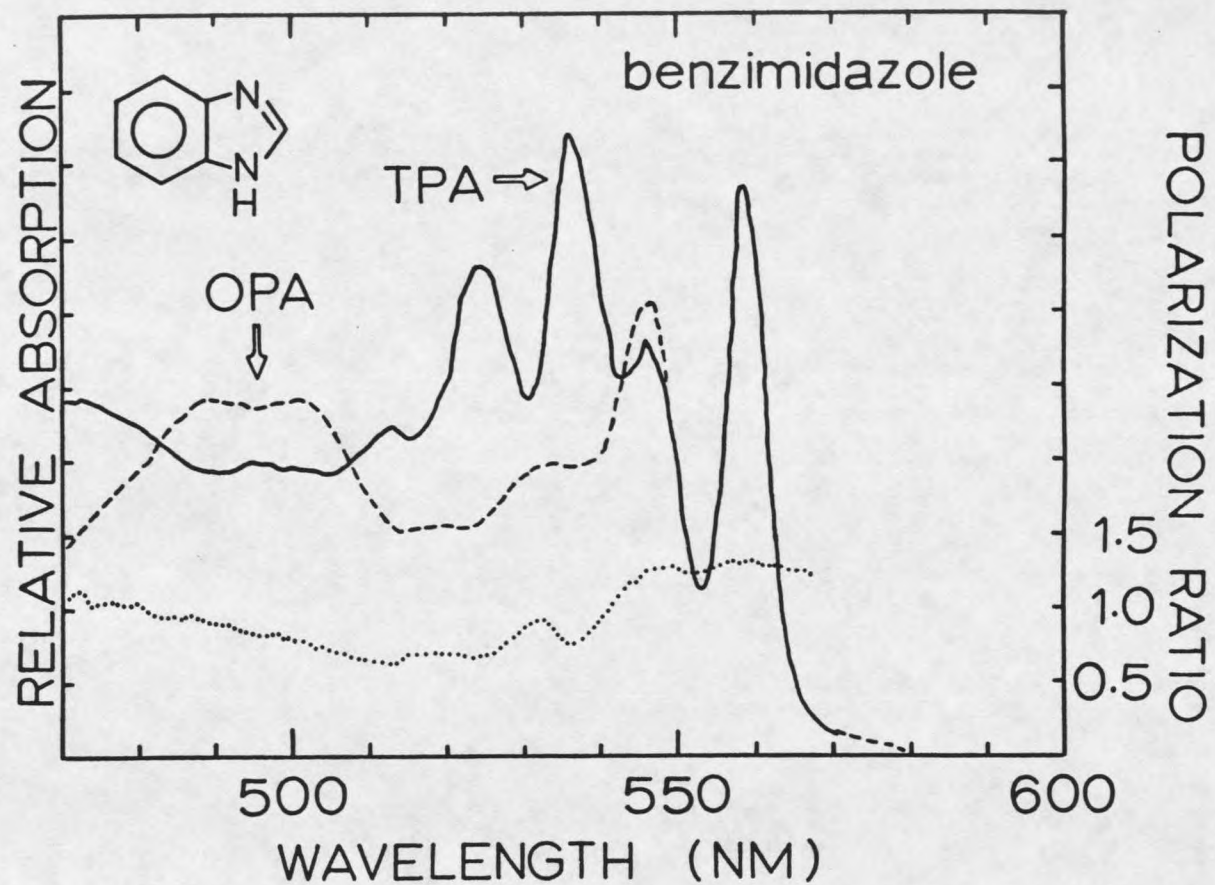


Figure 4: Two-photon fluorescence excitation (solid line), one photon absorption (dashed line), and two-photon polarization (dotted line) spectra for benzimidazole dissolved in isopropanol (0.2M).

appears. The polarization spectrum shows  $\Omega$  high for the 0-0 and 0-1 of  $L_B$  but a much lower polarization is exhibited by the new peaks. The behavior of these peaks indicates a vibronic origin. A smaller dip in the polarization spectrum between the 0-0 and 0-1 may also be due to a two-photon active vibrational mode. The  $L_a$  state appears to be reduced also for benzimidazole, and shows an  $\Omega$  slightly less than 1.0 while the  $L_B$  state shows  $\Omega = 1.3$ .

The data for the cation of benzimidazole (0.2m in methanol- $H_2SO_4$ ) is shown in Figure 5. Two peaks which do not appear in the one-photon absorption again appear at about  $0+1550\text{ cm}^{-1}$  with a spacing similar to that of the 0-0 and 0-1. The polarization spectrum shows a high  $\Omega$  value for the 0-0 and 0-1 peaks with dips corresponding to the two vibronic peaks. Interestingly, the polarization ratio falls on either side of the 0-0.

Figure 6 presents the two-photon spectra of each molecule such that the two-photon absorptivity scale is the same for each molecule. This graph was constructed using measurements of the relative  $\delta$ 's as outlined in the experimental section. The units are such that  $\delta = 1$  for toluene in cyclohexane excited at 513 nm ( $^*v_{14}$ ). Indole shows a two-photon absorptivity approximately five times that for toluene. The benzimidazoles are only slightly stronger than toluene.

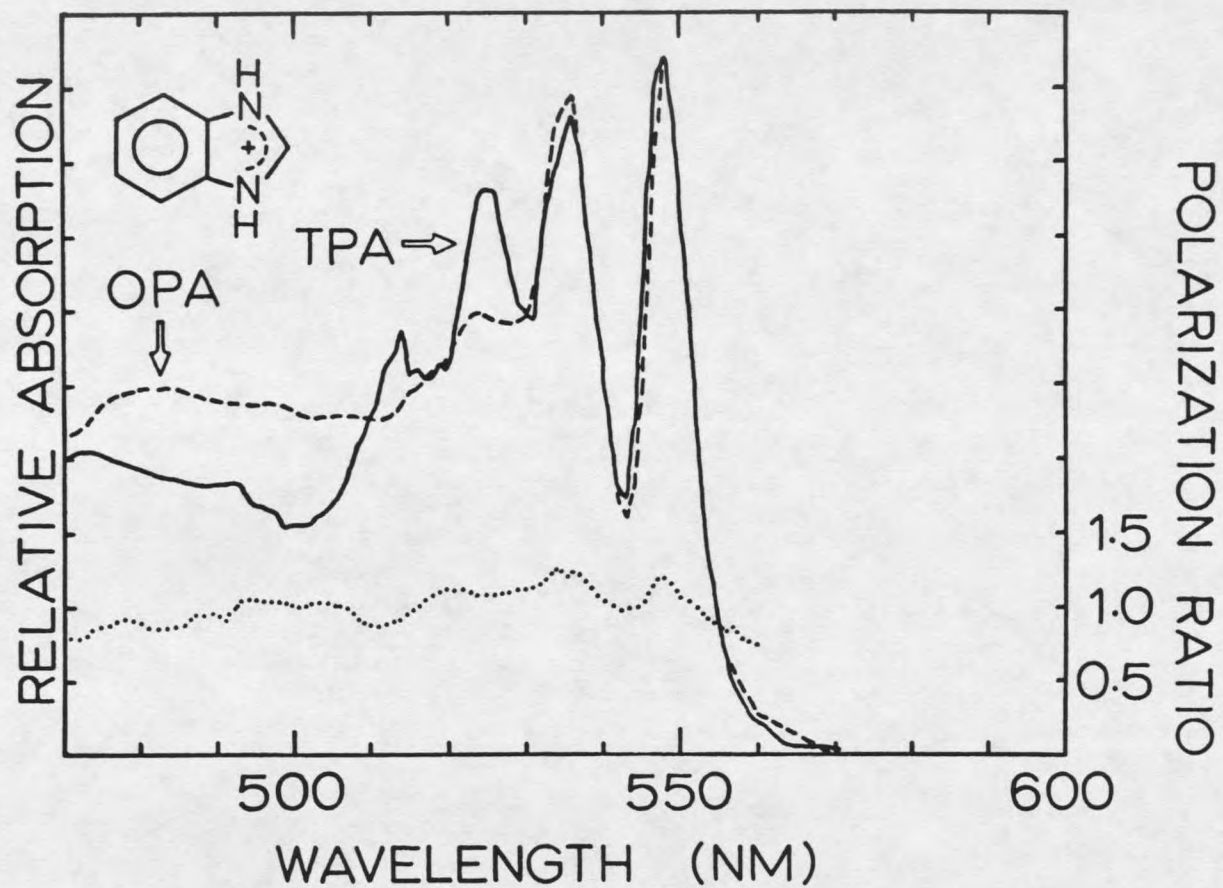


Figure 5: Two-photon fluorescence excitation (solid line), one photon absorption (dashed line), and two-photon polarization (dotted line) spectra for benzimidazole dissolved in methanol + H<sub>2</sub>SO<sub>4</sub> (0.2M).

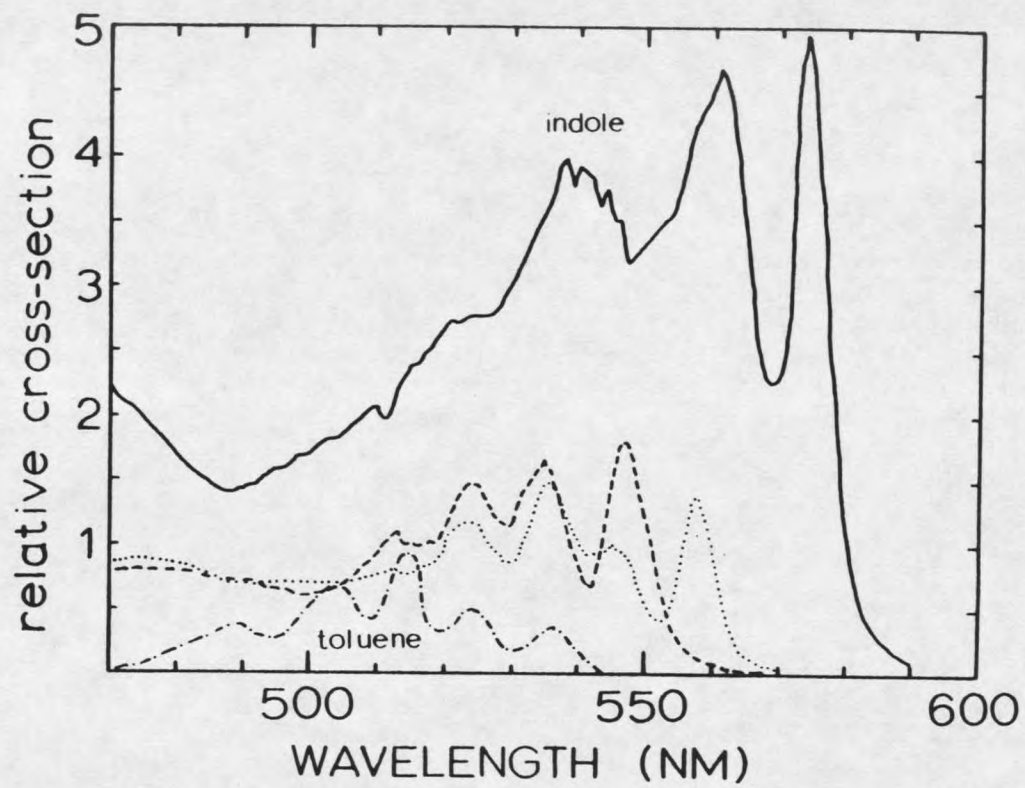


Figure 6: Relative two-photon absorptivities for indole, benzimidazole, benzimidazole cation, and toluene.

DiscussionIndole

The degenerate  $L_a$  and  $L_b$  bands of indole have been the subject of intensive study (4,53), yet much remains unknown because they do overlap so extensively. A greater sensitivity to solvent environment for the  $L_a$  state, believed due to its larger dipole (16,17,54,55), has been the basis for assigning peaks to  $L_a$  or  $L_b$  in absorption. (7,8,22) The solvent shift technique utilized by Strickland and co-workers has led them to assign a peak at about 1000  $\text{cm}^{-1}$  above the  $L_b$  0-0 to the  $L_a$  0-0 for indole in methylcyclohexane. The two-photon results are largely consistent with this assignment. Assuming a 500  $\text{cm}^{-1}$  fwhm for this peak the polarization ratio should begin dropping at 567 nm but it is seen to be dropping already at 572 nm. It may be that the  $L_a$  0-0 is much broader than assumed or is somewhat closer to the  $L_b$  0-0 than previously believed. Nonetheless,  $L_a$  absorption begins very close to the  $L_b$  0-0. The structured fluorescence of indole in cyclohexane (Figure 7) is consistent with assigning  $L_b$  as the lowest state as indicated by the polarization spectrum.

The computed two-photon properties of indole are in good agreement with the experiment (see Table 1). The  $L_b$  state is predicted to show  $\Omega = 1.5$ , close to that observed. The low  $\Omega$  observed for the  $L_a$  state is also predicted

Table 1. INDO/s results for indoles studied. a) 10 x 20 singles only, Mataga-Nishimoto  $\delta$ 's; b) 14 x 14 singles only Mataga-Nishimoto  $\delta$ 's; c) 9 x 7 singles and doubles Ohno-Klopman  $\delta$ 's.

Derivative	$\Omega L_a$	$\Omega L_b$	$\delta_g + \delta_n$ ( $L_b$ , gm)	$\delta_g + \delta_n$ ( $L_a$ , gm)	$E_{L_a} - E_b$ ( $\text{cm}^{-1}$ )
5MI	a) 1.498	0.578	125.573	163.883	4478.6
	b) 1.499	0.583	117.187	169.828	4680.28
	c) 1.497	0.372	24.939	31.889	6255.34
Indole	a) 1.494	0.479	89.846	131.537	3367.90
	b) 1.496	0.468	92.139	164.805	3905.01
	c) 1.497	0.324	12.230	27.693	6584.31
1MI	a) 1.471	0.342	86.437	122.675	3178.50
	b) 1.471	0.350	82.600	138.356	3521.53
	c) 1.378	0.256	15.884	21.326	4734.45
2,3MI	a) 1.480	0.666	137.680	574.880	2946.6
	b) 1.480	0.664	131.630	583.676	2909.50
	c) 1.470	0.500	21.724	81.104	4594.01
3MI	a) 1.480	0.515	116.772	278.827	3021.90
	b) 1.474	0.526	108.867	301.672	3233.66
	c) 1.409	0.411	21.2269	33.700	5062.89
4MTI	a) 1.499	0.834	210.723	120.717	3794.30
	b) 1.498	0.809	205.696	123.411	3942.25
	c) 1.499	1.456	32.320	10.499	6067.99
5MTI	a) 1.495	0.588	156.411	168.303	4938.60
	b) 1.499	0.588	153.251	164.184	5069.59
	c) 1.497	0.429	33.337	55.458	6858.83
6MTI	a) 1.417	0.265	92.654	73.062	4217.50
	b) 1.413	0.266	85.594	76.229	4320.20
	c) 1.433	1.099	17.966	90.040	6233.78
7MTI	a) 1.500	0.449	43.341	115.672	4137.21
	b) 1.499	0.464	40.471	121.477	4305.43
	c) 1.468	0.369	12.131	40.816	5844.24

successfully. It should be noted that unless the ground and final states are included in the sum over intermediate

states, the  $L_a$  polarization ratio is predicted to be near 1.5. The charge transfer character and associated dipole moment change for the  $L_a$  state contribute to the  $xx$  and  $xy$  terms of the two-photon tensor and lead to the low  $\Omega$  value. The ground and final states of this polar molecule contribute because the  $L_a$  transition moment and the dipole moment change are largely in the  $x$  direction. Such a contribution has been predicted theoretically (39) and this may represent the first experimental observation. INDO/S predicts the two-photon absorptivity of indole to be about 10 times that for benzene, also in good agreement with the results.

#### Benzimidazole

Perhaps the most interesting feature of the two-photon spectrum of benzimidazole is the appearance of two vibronic peaks without analog in the one-photon spectrum. These peaks are assigned to a vibration similar to the  $\nu_{14}$  vibration of benzene and the  $\nu_{21}$  vibration of naphthalene (56) that is so effective in inducing two-photon intensity. A vibration that distorts the six-membered ring of benzimidazole toward a kekule structure is predicted by a normal mode calculation, FORCE, based on an MNDO generated force field (57). The ground state frequency is calculated to be  $1302 \text{ cm}^{-1}$  and agrees with the analysis by Cordes and Walter (58) who find  $1316 \text{ cm}^{-1}$  and assign the IR band observed at  $1280 \text{ cm}^{-1}$  to this vibration. An increase

similar to the  $300 \text{ cm}^{-1}$  increase in the  $\nu_{14}$  frequency for the excited  $L_b$  state of benzene would bring the frequency to about  $1580 \text{ cm}^{-1}$ , in close agreement with that observed.

The INDO/S calculations are somewhat less successful for benzimidazole in that the calculated  $\delta g + \delta h$  values are about three times higher than observed. Also, the  $L_b$  of benzimidazole is predicted to be of the same absorptivity as indole's  $L_b$  and appears not to be the case. The calculations predict  $\Omega_b = 1.33$  and  $\Omega_{L_a} = 1.23$  which is consistent with what is observed since the  $L_a$  state is overlapped by states with low polarization on both sides.

#### Benzimidazole Cation

In addition to the interesting vibronic peaks shown for this molecule, benzimidazole cation shows a very interesting polarization spectrum.  $\Omega$  is high only at the first two  $L_b$  peaks and low elsewhere. The drop in polarization seen on the red edge of the excitation spectrum is interesting in light of the large red shift in fluorescence maximum seen for the benzimidazole cation (59,60). Protonation of benzimidazole shifts the fluorescence maximum from 299 nm to 360 nm. Associated with this large Stokes shift is a loss of structure much like that observed for indole dissolved in water (6). The two lowest states of the cation are predicted to have charge transfer character like the  $L_a$  state of indole. In the cation, the  $L_b$  state appears to have moved closer (blue shift) to the  $L_a$  state and may

actually allow  $L_a$  to become lowest. It is however possible that another state not predicted by the theory underlies the structured  ${}^1L_b$ . Tway and Love (60) have proposed that prototropic equilibria in the excited state explain the charge transfer type fluorescence seen in certain benzimidazole and thiabenzimidazole homologues. INDO/s certainly fails in regard to the predicted absorptivity for the cation. It is calculated to be 20 to 40 times that of benzene.

#### Summary

Two-photon spectroscopy of three nine-membered ring systems has provided a mechanism by which to further test the semi-empirical methods relied upon for insight in these systems. INDO/S does a good job predicting the two-photon properties of indole but fails for the benzimidazoles, especially the cation. The large difference in  $\Omega$  of the  $L_a$  and  $L_b$  states of indole offers a method of resolving these two states in room temperature solvent systems as well as in the gas phase. The data for indole in cyclohexane are consistent with literature assignments of the  $L_b$  state as the lowest singlet state with  $L_a$  about  $1000\text{ cm}^{-1}$  above it in hydrocarbon solvent.

## SOLVENT AND SUBSTITUENT EFFECTS ON INDOLE

Background

The effect of environment on the fluorescence characteristics of indoles forms the basis for interpretation of protein fluorescence spectra. Solvation is the most obvious and thoroughly studied perturbation of the indole ring. (4) Substituted indoles (see Figure 7), with their varying  $L_a$ - $L_b$  energy gaps, have served as models for the study of solvation effects on the  $L_a$  and  $L_b$  states. For most methyl derivatives, polar solvation leads to a loss

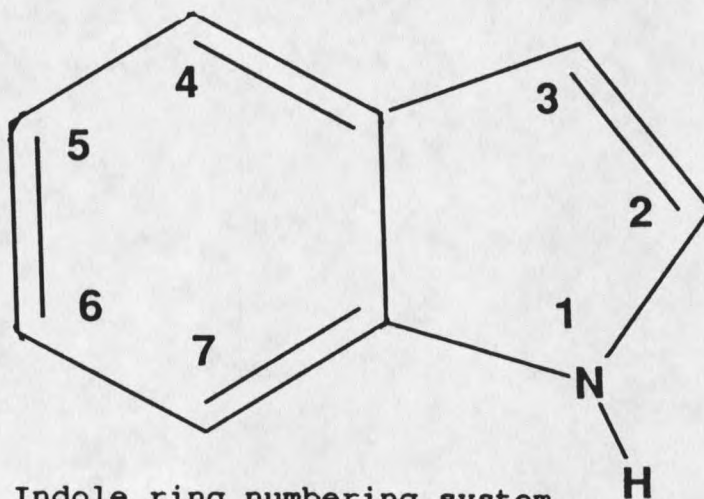


Figure 7: Indole ring numbering system.

of structure and a large red shift of the fluorescence. This drastic change in fluorescence behavior is accompanied by only small changes in absorption. The fluorescence changes, moreover, begin to occur for solutions containing very small amounts of polar solvent in hydrocarbon. Specific interactions between indoles and polar solvents are

implicated by this behavior. As the concentration of polar solvent is increased, the fluorescence slows its broadening and only shifts further to the red. Experiments in viscous polar solvents, where the solvent relaxation time is comparable to the fluorescence lifetime, show that the fluorescence undergoes a red-shift in time due to solute-solvent relaxation (SSR) (68). In rigid polar glasses where SSR cannot occur the fluorescence loses much of its red shift and becomes somewhat structured. These results suggest that a non-specific interaction is responsible for the red shift. Various theories have drawn upon specific and non-specific interactions alike to explain the anomalous fluorescence behavior of indoles in polar solvents.

Van Durren (15) discussed the role of solvent dielectric and hydrogen bonding on indole fluorescence, citing non-specific dielectric properties as more important. Mataga, et al. (16) proposed that a reversal of the  $L_a$  and  $L_b$  levels during the excited lifetime of indole was responsible for the red shift. In their model, a large increase in dipole moment upon excitation initiates solvent relaxation which preferentially stabilizes the larger dipole moment of the  $L_a$  state. Similar models have been proposed by Song & Kurtin (18) and Suzuki et al. (17). Mataga et al. also predicted that the  $L_a$  state of indole should have a large contribution from a configuration resembling styrene's lowest charge transfer (CT) state. Furthermore, they stated

that the contribution of this configuration would likely increase as a result of the interactions with the polar solvent during the excited state lifetime.

Based upon the specific nature of the polar interaction, Lumry and co-workers have, in a series of papers (13,61-64), proposed the existence of excited state solute-ground state solvent complexes ("exciplexes") which stabilize charge centers in the excited state by dipole-dipole interactions. These exciplexes were shown to exhibit 1:1 and/or 1:2 stoichiometry and are believed to involve complexation at N-1 and C-3 of the indole ring. 5-methoxyindole was classified as a non-exciplex forming indole since polar solvation produces no greatly red-shifted fluorescence for this molecule. The exciplex model does however neglect the relative  $L_a$ - $L_b$  energy gap and the state of origin for the red-shifted fluorescence. Another specific interaction deduced for indoles and used to explain the anomalous fluorescence characteristics is that of ground state complexes. Skalski et al. (14) were able to correlate changes in absorption with the appearance of a red-shifted component in the fluorescence for 1-methylindole.

Virtually all of the work on the nature of the fluorescent state of indoles in polar solvents has based its explanation of experimental results on at least one of the aforementioned proposals; i.e., SSR around the large dipole of  $L_a$ , charge transfer, level inversion, exciplex formation,

and ground state complexes. Hydrogen bonding to the indole N-H group has been somewhat ignored as an explanation. This is likely due to the similar photophysics of 1-methylindole. The more recent fluorescence solvent shift studies of  $L_a$ mi have led to a model which includes ground state complexes and  $L_a$ - $L_b$  level inversion as a result of both solvent polarity and solvent reorientation. The growing charge transfer character for  $L_a$  due to SSR during the excited state lifetime has been re-emphasized by the time-resolved fluorescence experiments of Meech et al. (19). It is in a synthesis of the above models that a truer picture of indole photophysics has emerged.

Important to interpretation in terms of these models is the relative energy of the  $L_a$  and  $L_b$  states. This is especially true for derivatives with closely spaced levels where dual emission from  $L_a$  and  $L_b$  is possible. While the broadening of the  $L_a$  and  $L_b$  absorption peaks in polar solvents make their assignment difficult, it is even more difficult to discern the onset of  $L_a$  absorption which is apparently so important in describing the anomalous fluorescence. Polarized two-photon fluorescence excitation spectroscopy provides a direct method of viewing the  $L_a$  and  $L_b$  states separately despite their large degree of overlap.

It is the aim of this section to describe efforts in following the movement of the  $L_a$  and  $L_b$  states under the influence of polar solvation for a series of methyl and

methoxy derivatives of indole. As a reference point, two-photon spectra of the compounds dissolved in cyclohexane were obtained. These are then compared to those observed in n-butanol. The two-photon spectra, especially the  $\Omega$  spectra, provide a firm basis on which to discuss the proposed models of indole fluorescence. The absorption and fluorescence changes upon polar solvation were recorded as an aid in the discussion. The results of INDO/S calculations for the derivatives are also presented as they lend insight and support.

### Two-Photon Spectra

#### Indoles in Cyclohexane

5-methylindole (5MI). Of all the methylindoles, 5-methylindole (Figure 8, 0.01M cyclohexane) shows the largest  $L_a$ - $L_b$  energy gap (9). The structured  $L_b$  state is well separated from the broad  $L_a$  state in both the one-photon absorption (OPA) (dashed lines) and the two-photon excitation spectra (TPA) (solid line). The polarization spectrum ( $\Omega$ ) (dotted line) shows a high value of  $\sim 1.3$  for the  $L_b$  0-0 and is still above 1.0 for the  $L_b$  0-1. It then drops to  $\sim 0.6$  for shorter wavelength excitation and then rises again to the blue as a third transition with a higher polarization ratio is excited below 510 nm.

Indole. Presented again (Figure 9, 0.01M in cyclohexane) but this time at a slightly lower concentration

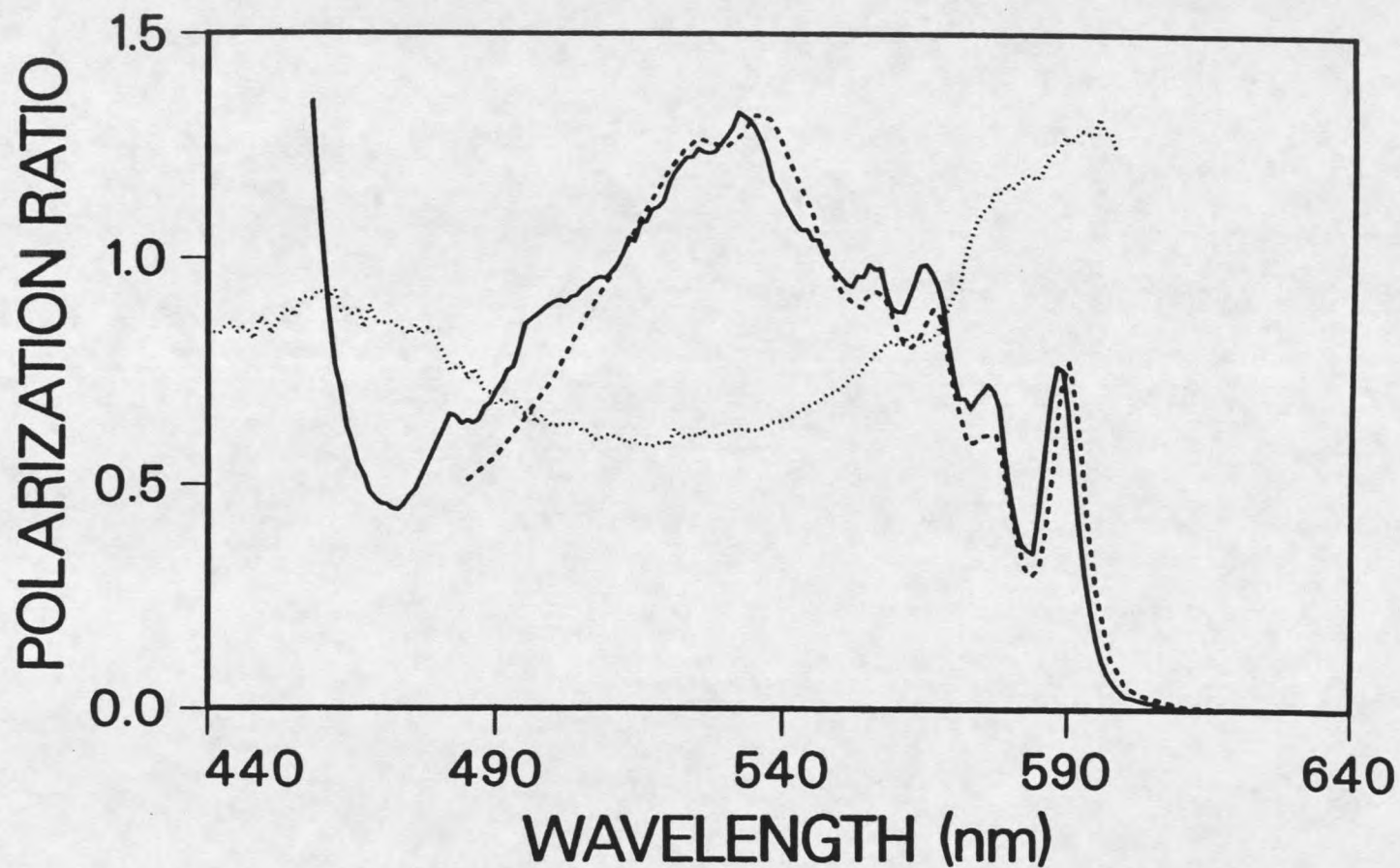


Figure 8: Two-photon fluorescence excitation (solid line), one photon absorption (dashed line), and two-photon polarization (dotted line) spectra for 5-methylindole dissolved in cyclohexane (0.01M).

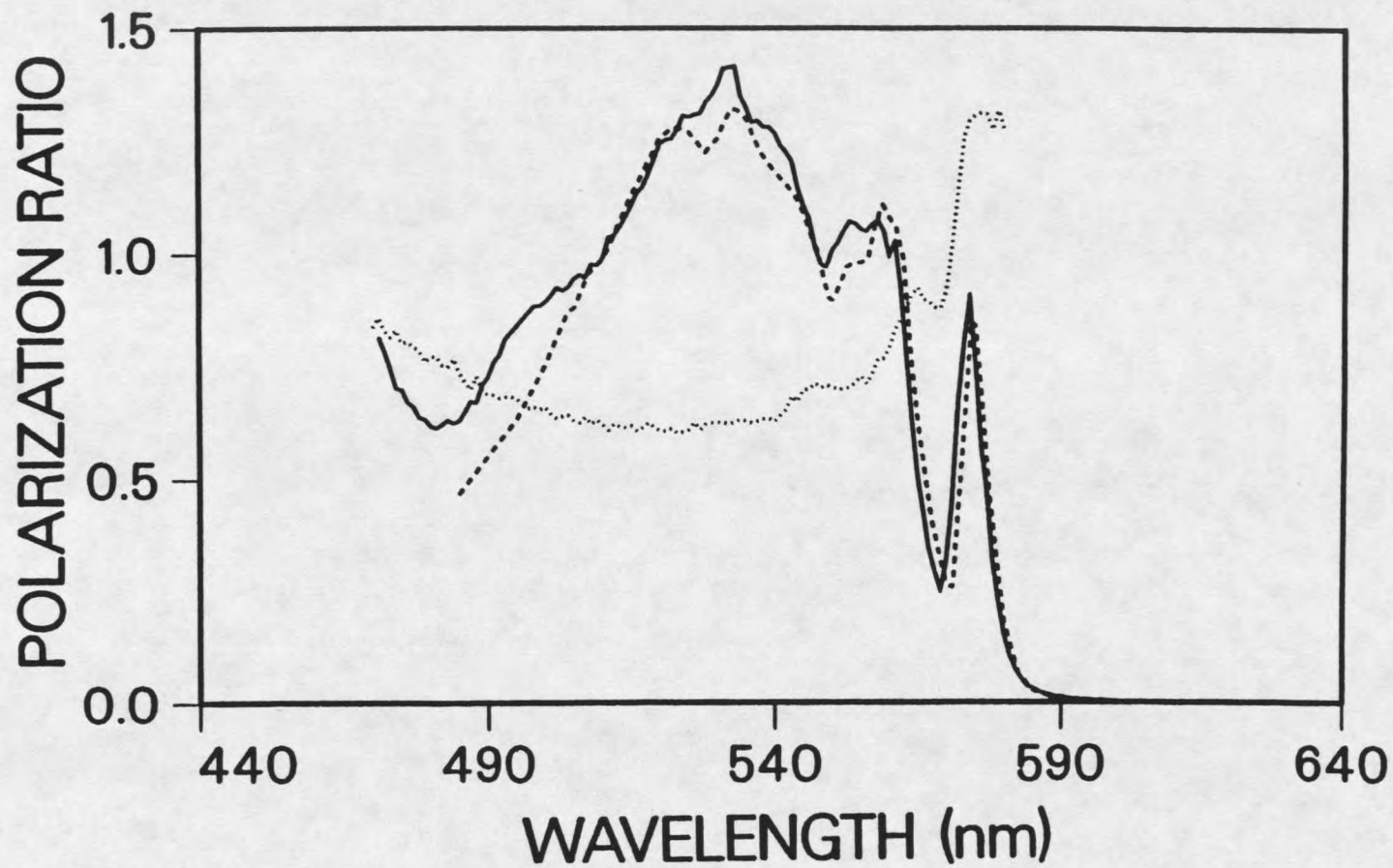


Figure 9: Two-photon fluorescence excitation (solid line), one photon absorption (dashed line), and two-photon polarization (dotted line) spectra for indole dissolved in cyclohexane (0.01M).

the profile seen with the YAG system, the TPA is seen to follow the OPA closely like the TPA of 5-methylindole. The polarization spectrum is identical to that shown before for the 0.05M solution with  $\Omega \sim 1.4$  at the origin and dropping steeply to the blue where it levels off at  $\Omega \sim 0.65$  for bulk  $L_a$  excitation. Again, a third transition with a higher  $\Omega$  value begins to absorb below 510 nm.

1-methylindole (1MI). Figure 10 shows the results for 1-methylindole (0.01 M cyclohexane). This molecule is believed to have a somewhat smaller  $L_a-L_b$  energy gap than indole (12) and the  $\Omega$  spectrum is consistent with  $L_a$  being closer in energy to the  $L_b$  0-0. The  $\Omega$  value at the origin is just above 1.1 and drops steeply in the region between the  $L_b$  0-0 and 0-1 which are still resolved. The polarization ratio for what should be  $L_a$  excitation drops only to about 0.8. The third transition, growing in below 520 nm, shows a polarization ratio above 1.1. The high polarization ratio for  $L_a$  excitation may be a reflection of the fact that 2 states with high  $\Omega$  values straddle it on both sides and seems to indicate that  $L_a$  may be somewhat reduced in this molecule despite the apparent TPA.

3-methylindole (3MI). 3-methylindole (Figure 11, 0.01M cyclohexane) is the most closely related to tryptophan (also 3-substituted) and is believed to have the  $L_b$  0-0 and  $L_a$  0-0 superposed in hydrocarbon (7). This would account for the strength of the origin peak relative to the rest of the

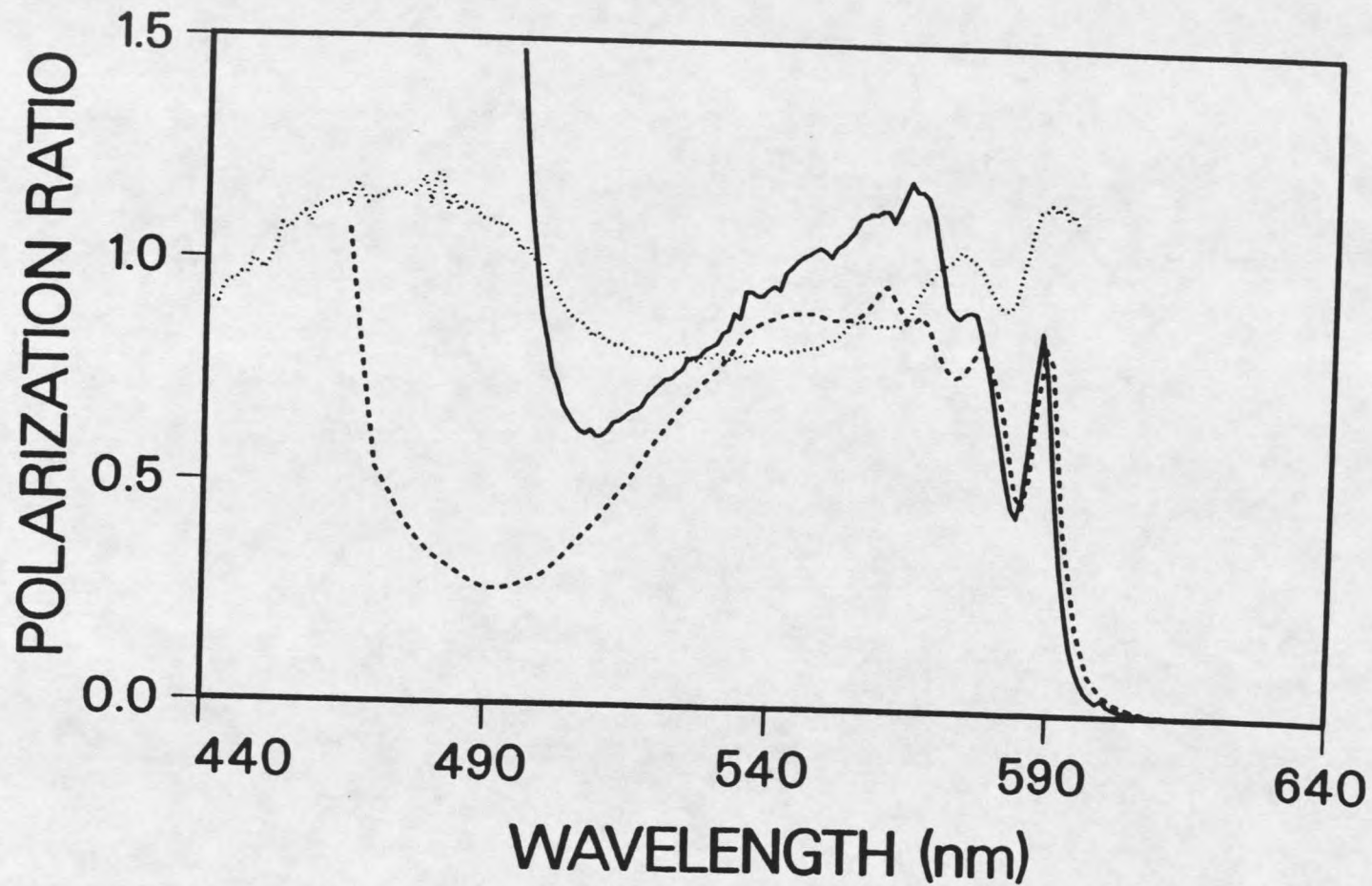


Figure 10: Two-photon fluorescence excitation (solid line), one photon absorption (dashed line), and two-photon polarization (dotted line) spectra for 1-methylindole dissolved in cyclohexane (0.01M).

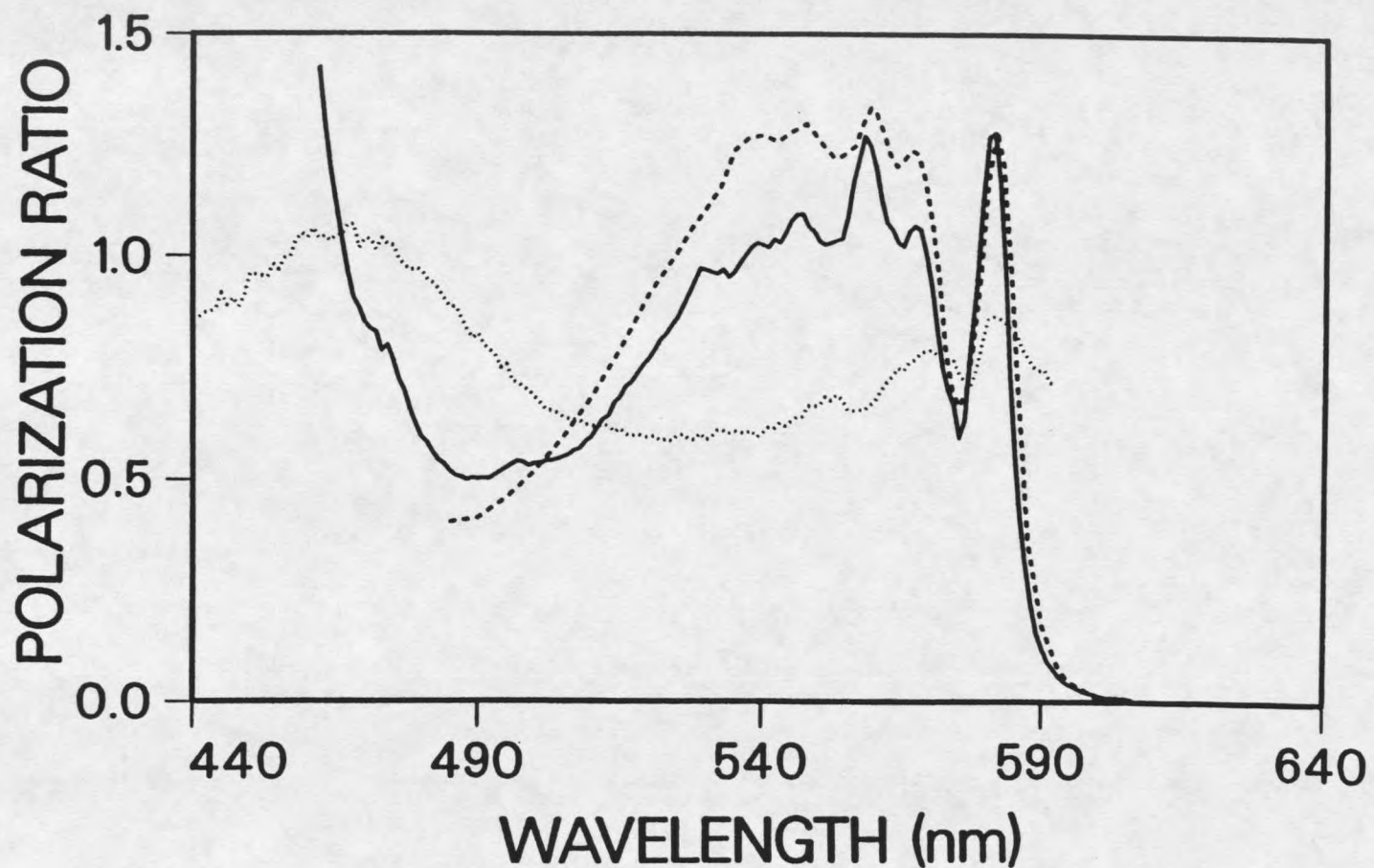


Figure 11: Two-photon fluorescence excitation (solid line), one photon absorption (dashed line), and two-photon polarization (dotted line) spectra for 3-methylindole dissolved in cyclohexane (0.01M).

absorption in both the OPA and TPA. The  $\Omega$  value of only 0.9 at the origin also hints that this is the case. The polarization ratio drops on the red edge indicating that the  $L_a$  0-0 is somewhat broader than the  $L_b$  0-0. Like 1-methylindole, the rise in  $\Omega$  for the 0-1 peak of  $L_b$  is broader than is seen for indole. This may be a manifestation of the  $L_b$  0+730  $\text{cm}^{-1}$  and 0+980  $\text{cm}^{-1}$  peaks seen for indole and 3-methylindole by Strickland (7).  $L_a$  may also in fact be reduced for this molecule and the TPA seems to indicate this is true. A prominent peak appearing at 558 nm in the TPA has a dip in the polarization spectrum associated with it and surely is part of the  $L_a$  manifold. Strickland tentatively assigned this peak in OPA as  $L_b$  0+1340  $\text{cm}^{-1}$ . It appears it may be a superposition of an  $L_a$  peak and an  $L_b$  peak.  $L_a$  excitation gives an  $\Omega$  value of about 0.6 and again a third transition with high  $\Omega$  grows in below 510 nm.

2,3 dimethylindole (2,dMI). The 2,3 dimethyl substituted derivative (Figure 12, 0.01M cyclohexane) exhibits the smallest  $L_a$ - $L_b$  energy gap (8). In fact, this molecule is believed to have  $L_a$  lowest even in the vapor state (65). The polarization ratio is  $\sim 0.5$  on the red edge and a shoulder is visible in the TPA. Strickland has assigned this shoulder in OPA as the 0-0  $L_a$ . An intrinsic polarization ratio of 0.5 can thus be assigned to the  $L_a$  state; very different from the  $\Omega=1.4$  found for the  $L_b$

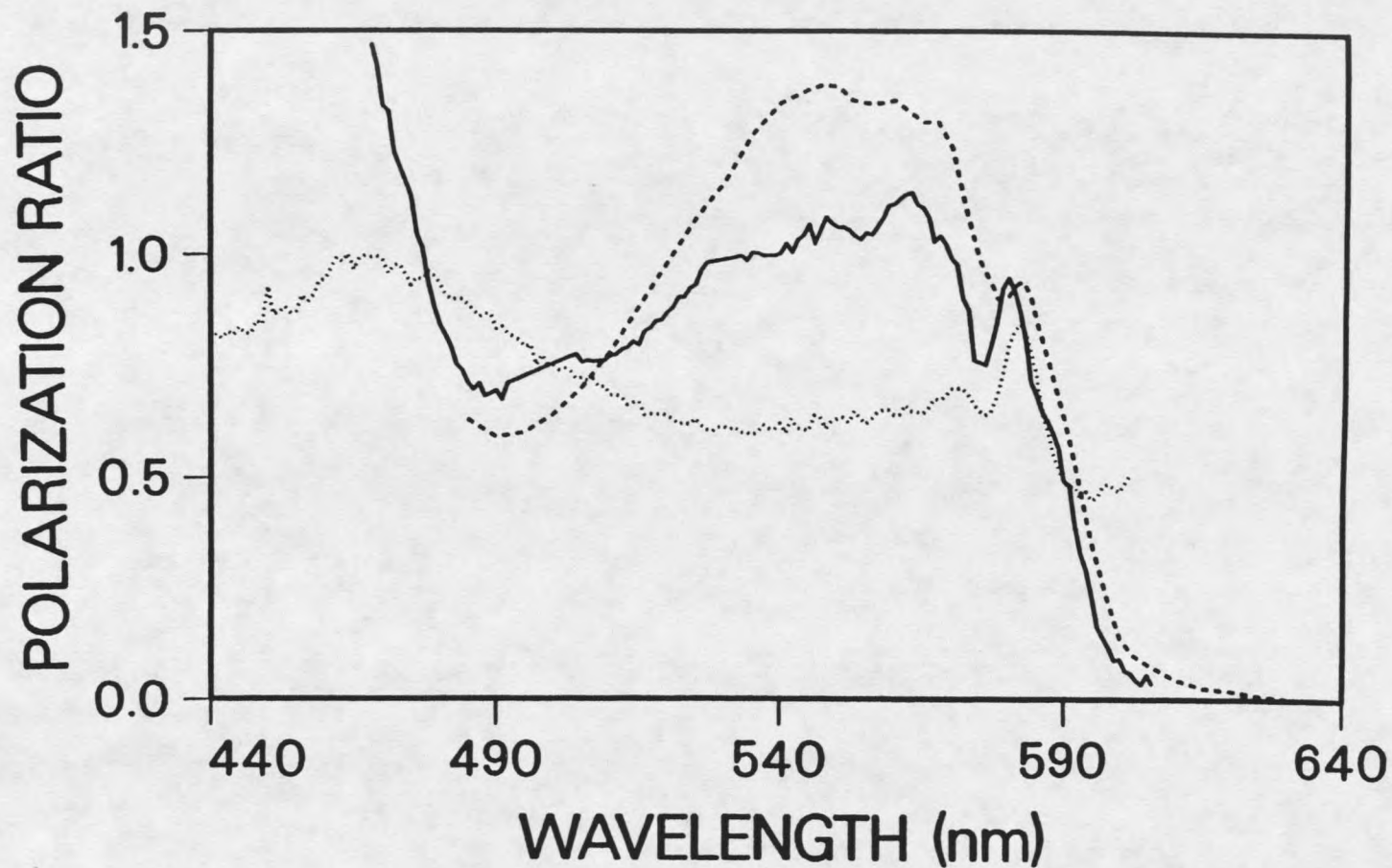


Figure 12: Two-photon fluorescence excitation (solid line), one photon absorption (dashed line), and two-photon polarization (dotted line) spectra for 2,3-dimethylindole dissolved in cyclohexane (0.01M).

state. The  $L_b$  origin peak shows  $\Omega=0.85$  and excitation of  $L_a$  gives an  $\Omega$  of about 0.6. Overlap of  $L_a$  with the  $L_b$  state and the third transition seen again must contribute to the somewhat higher  $L_a$   $\Omega$ .

4-Methoxyindole (4MTI). The one and two-photon spectra of 4-methoxyindole in cyclohexane (.004M) are shown in Figure 14. The  $\Omega$  value of 1.45 for the origin of this molecule is the highest observed and is quite close to the theoretical maximum. The polarization ratio begins to fall after the 0-1 of the  $L_b$  to a low value of 0.85. A conspicuous dip at 552 nm probably corresponds to the 0-0 of the  $L_a$  state. 4-methoxyindole is predicted to have a much reduced intensity for the  $L_a$  state (Table 1). The TPA and the high  $\Omega$  value for  $L_a$  excitation support this picture. The third transition again appears to the blue and may also contribute to the high  $\Omega$ .

5-methoxyindole (5MTI). The 5-methoxy derivative (0.004M cyclohexane) exhibits the largest separation of the  $L_a$  and  $L_b$  states seen (Figure 14). The structured  $L_b$  state exhibits a high polarization ratio of about 1.25 for the first three peaks visible. Substitution at the 5-position apparently lowers the  $\Omega$  value of the  $L_b$  state. The 5-methyl derivative (Figure 8) also has a somewhat lower value of  $\Omega$   $L_b$  than is seen for indole. The  $L_b$  state of 5-methoxyindole also shows another sign of being quite perturbed relative to indole's  $L_b$ . A shoulder appears at

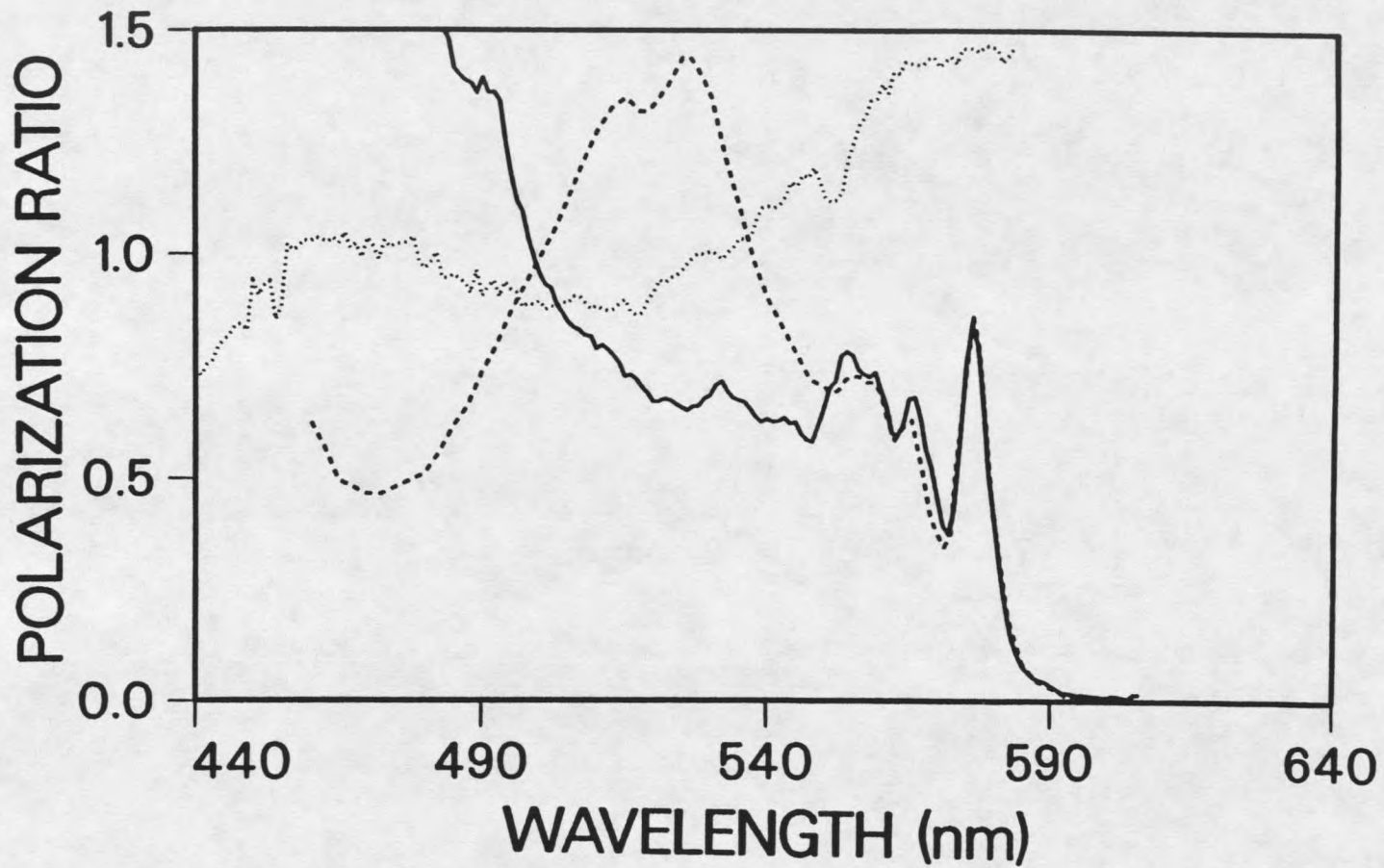


Figure 13: Two-photon fluorescence excitation (solid line), one photon absorption (dashed line), and two-photon polarization (dotted line) spectra for 4-methoxyindole dissolved in cyclohexane (0.004M).

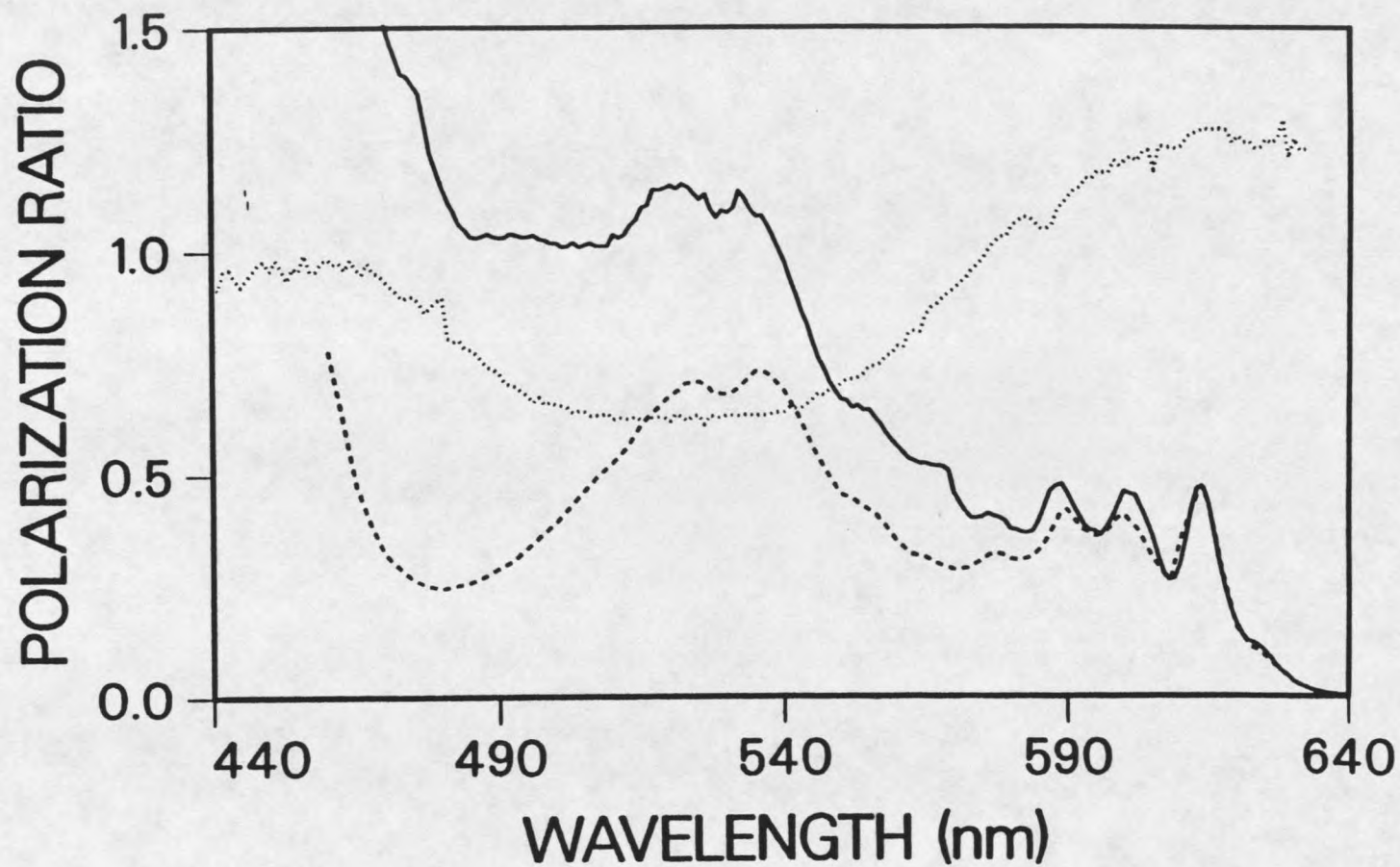


Figure 14: Two-photon fluorescence excitation (solid line), one photon absorption (dashed line), and two-photon polarization (dotted line) spectra for 5-methoxyindole dissolved in cyclohexane (0.004M).

about 623 nm in TPA and 311nm in OPA which is not observed for the other derivatives. This peak was assigned as a hot band by Strickland (9) but this does not appear to be true. They cooled a sample to 90°K in polar solvent and saw that it had disappeared. The polar solvent has the effect of blurring all the transitions and the room temperature spectrum in n-butanol (see Figure 35) does not show the shoulder resolved either. The new assignment of the shoulder would be  $L_b$  0-0 which results in an  $L_b$  band shape much different than for indole. Such an alteration of the  $L_b$  band shape might be expected since the transition density pattern of the  $L_b$  state is mostly in the six ring (48). Another interesting feature appears in the  $\Omega$  spectrum at 587 nm where a reproducible dip like that seen in 4-methoxyindole apparently reveals the position of the  $L_a$  0-0 or a vibronic peak of  $L_b$ .  $L_a$  excitation gives a value of about 0.62 and the third transition grows in below 500 nm.

6-methoxyindole (6MTI). Like 4-methoxyindole, 6-methoxyindole (Figure 15, 0.004M cyclohexane) is predicted to have a much reduced  $L_a$  intensity (Table 1). The TPA indicates that this is true. Very little TPA intensity is seen in the wavelength region where  $L_a$  should appear. Unlike the other molecules studied, the TPA does not correspond well to the OPA. The TPA is seen to have a maximum at 563nm which does not have an analog in the OPA. Another peak in this new band appears at 573nm, and the

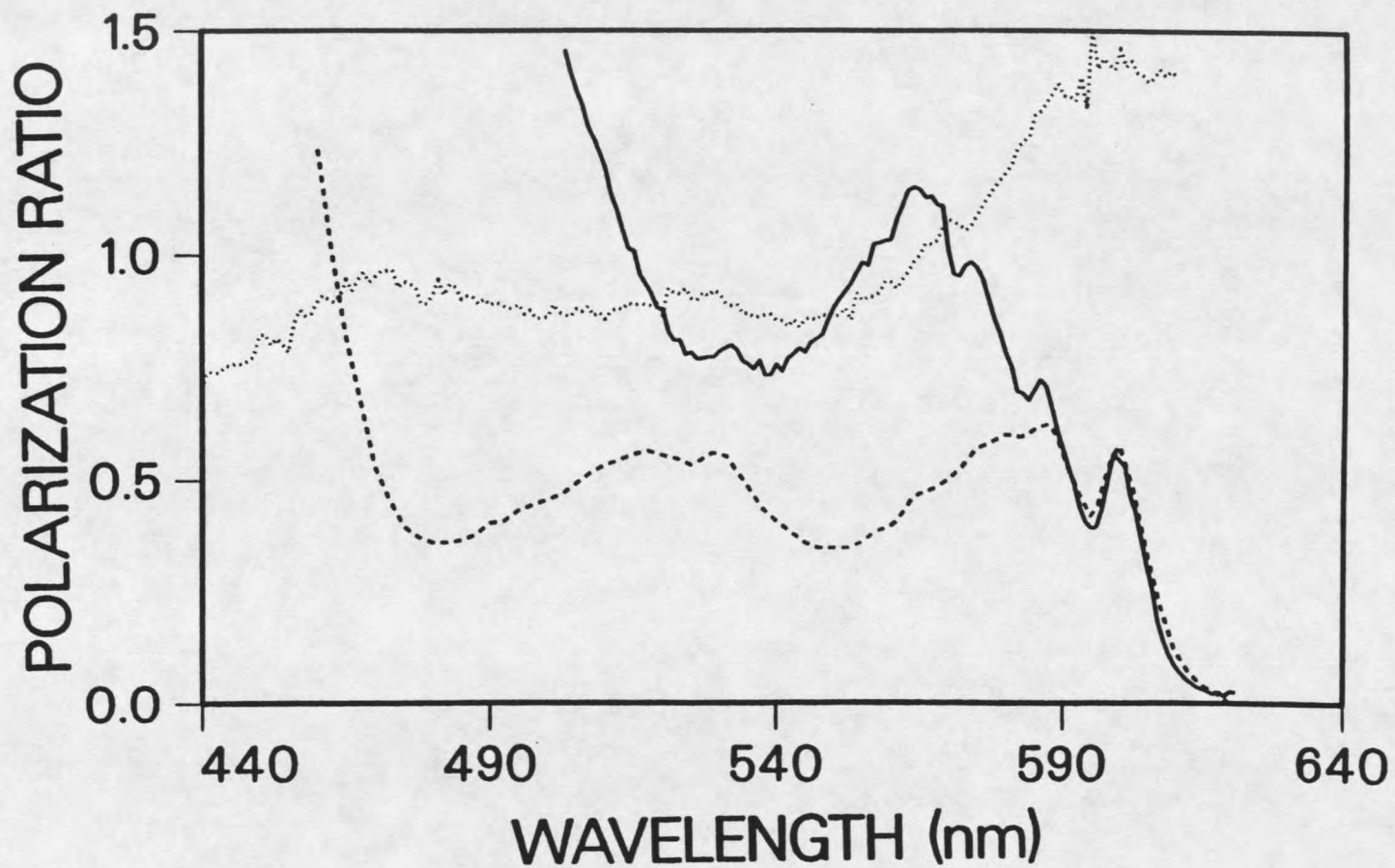


Figure 15: Two-photon fluorescence excitation (solid line), one photon absorption (dashed line), and two-photon polarization (dotted line) spectra for 6-methoxyindole dissolved in cyclohexane (0.004M).

separation of the 0-0 to this peak is  $1572\text{cm}^{-1}$ . In analogy to the benzimidazoles, this suggests a vibronic origin for the anomalous structure seen for this molecule. In the other indoles, the strongly allowed  $L_a$  covers up the vibronic structure. The strong third transition seems to cover  $L_a$  completely to the blue and  $L_b$  covers it to the red giving an  $L_a$   $\Omega$  value of 0.85. A slight rise in  $\Omega$  corresponding to the dip seen in the OPA at 525 nm belies  $L_a$ 's existence in the two-photon spectrum.

° 7-methoxyindole (7MTI). In contrast to 4 and 6-methoxyindole, for 7-methoxyindole (Figure 16, 0.04M cyclohexane) it is the  $L_b$  band which is predicted to be substantially reduced (Table 1). This would appear to be the case. The sharp origin peak is seen to have a polarization ratio that is lower ( $\Omega = 0.8$ ) than 2 peaks in  $\Omega$  that appear to the blue. The  $\Omega$  value for  $L_a$  excitation is 0.5, the value of  $\Omega$   $L_a$  in 2,3 dimethylindole where  $L_a$  is to the red of  $L_b$  and exposed. The low value of  $\Omega$  around 525 nm does seem to indicate that  $L_b$  is quite reduced for 7-methoxyindole but why does the origin have a low polarization? It is possible that like 5-methoxyindole, 7-methoxyindole has a very different  $L_b$  band shape and a lower intrinsic polarization ratio. Another possibility is that the  $L_a$  0-0 is superposed with the  $L_b$  0-0 and this leads to the low  $\Omega$  value.

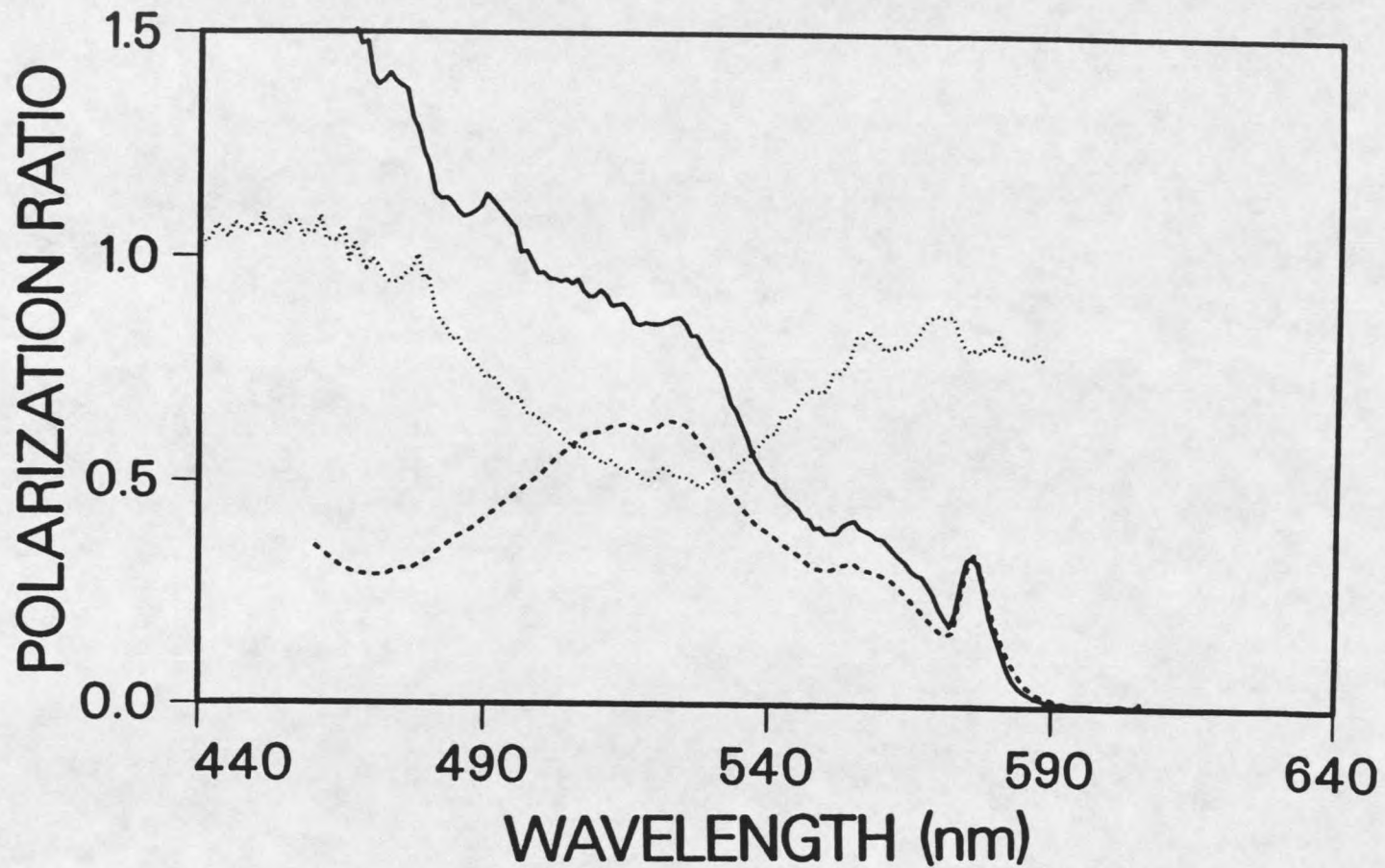


Figure 16: Two-photon fluorescence excitation (solid line), one photon absorption (dashed line), and two-photon polarization (dotted line) spectra for 7-methoxyindole dissolved in cyclohexane (0.004M).

Indoles in Butanol

5-methylindole. Figure 17 shows the TPA (solid line), the  $\Omega$  (dotted line), and the OPA (dashed line) for 5-methylindole dissolved in n-butanol at 0.01M. The main effect of polar solvation is to lower the polarization ratio at the origin and cause it to drop on the red edge. The polarization changes seen going from hydrocarbon by n-butanol are shown in Figure 18 and are consistent with a red shift of  $L_a$ . The fluorescence changes seen going to the polar solvent are shown in Figure 19 along with the absorption changes. The fluorescence maximum shifts from 310 nm in cyclohexane to 313 nm in butanol and the fluorescence becomes somewhat broader while losing structure in butanol.

Indole. The TPA,  $\Omega$ , and OPA for indole in butanol (0.01M) are shown in Figure 20. The polarization spectrum now closely resembles that seen for 3-methylindole in cyclohexane. Martinaud and Kadiri (10) have placed the 0-0  $L_a$  and 0-0  $L_b$  on top of one another for indole in polar solvents as a result of their solvent shift studies. The two-photon results suggest this is correct. The changes in the  $\Omega$  spectra for polar solvation are shown in Figure 21 and the associated absorption and fluorescence changes appear in Figure 22. Loss of structure in the fluorescence is accompanied by a shift in the maximum from 300 nm to 328 nm.

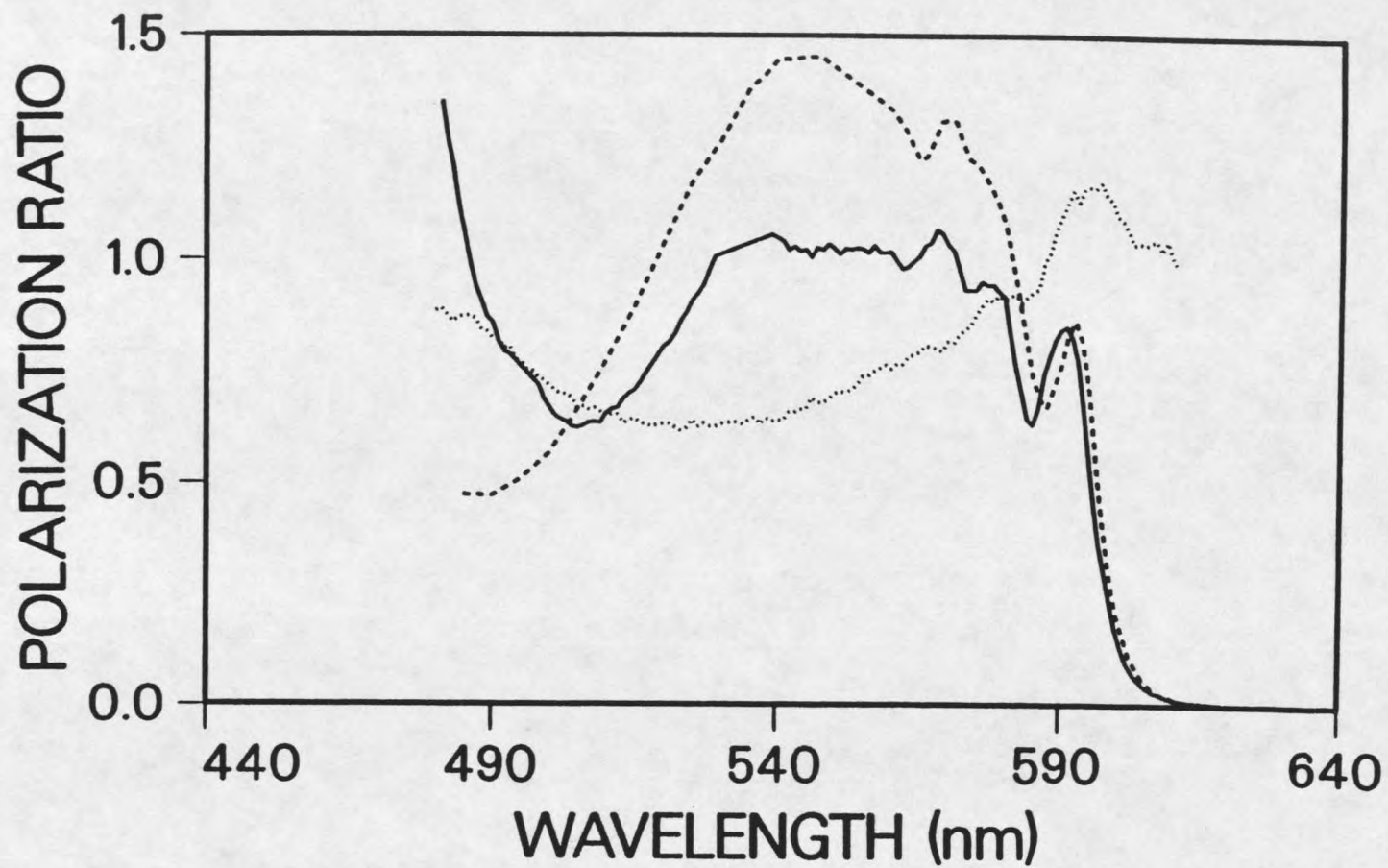


Figure 17: Two-photon fluorescence excitation (solid line), one photon absorption (dashed line), and two-photon polarization (dotted line) spectra for 5-methylindole dissolved in butanol (0.01M).

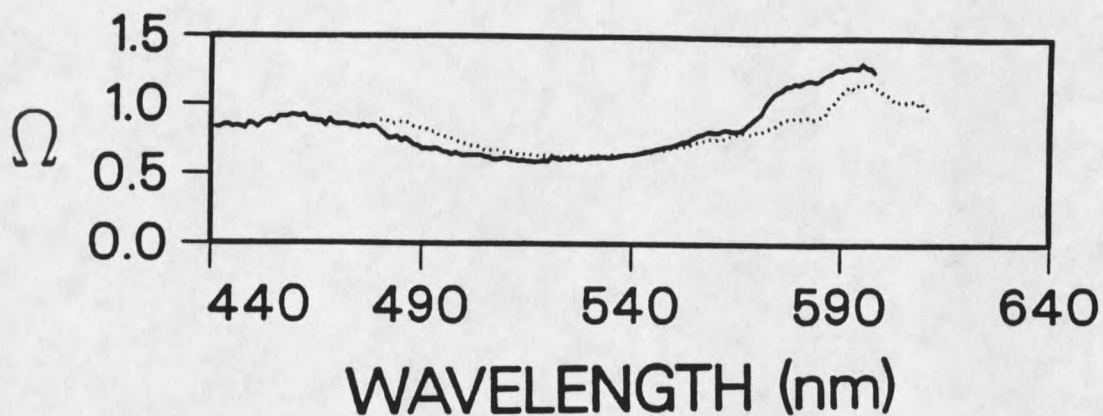


Figure 18: Two-photon polarization spectra of 5-methylindole in cyclohexane (solid line) and in butanol (dotted line) (0.01M).

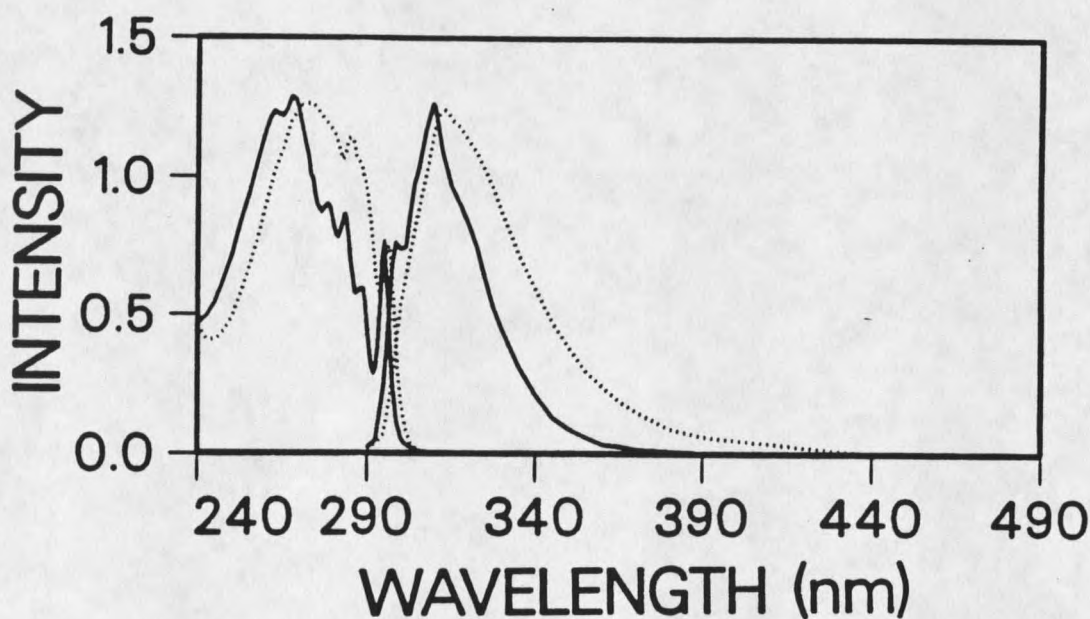


Figure 19: One-photon absorption and fluorescence spectra of 5-methylindole in cyclohexane (solid lines) and in butanol (dotted lines) ( $\sim 10^{-5}$ M).

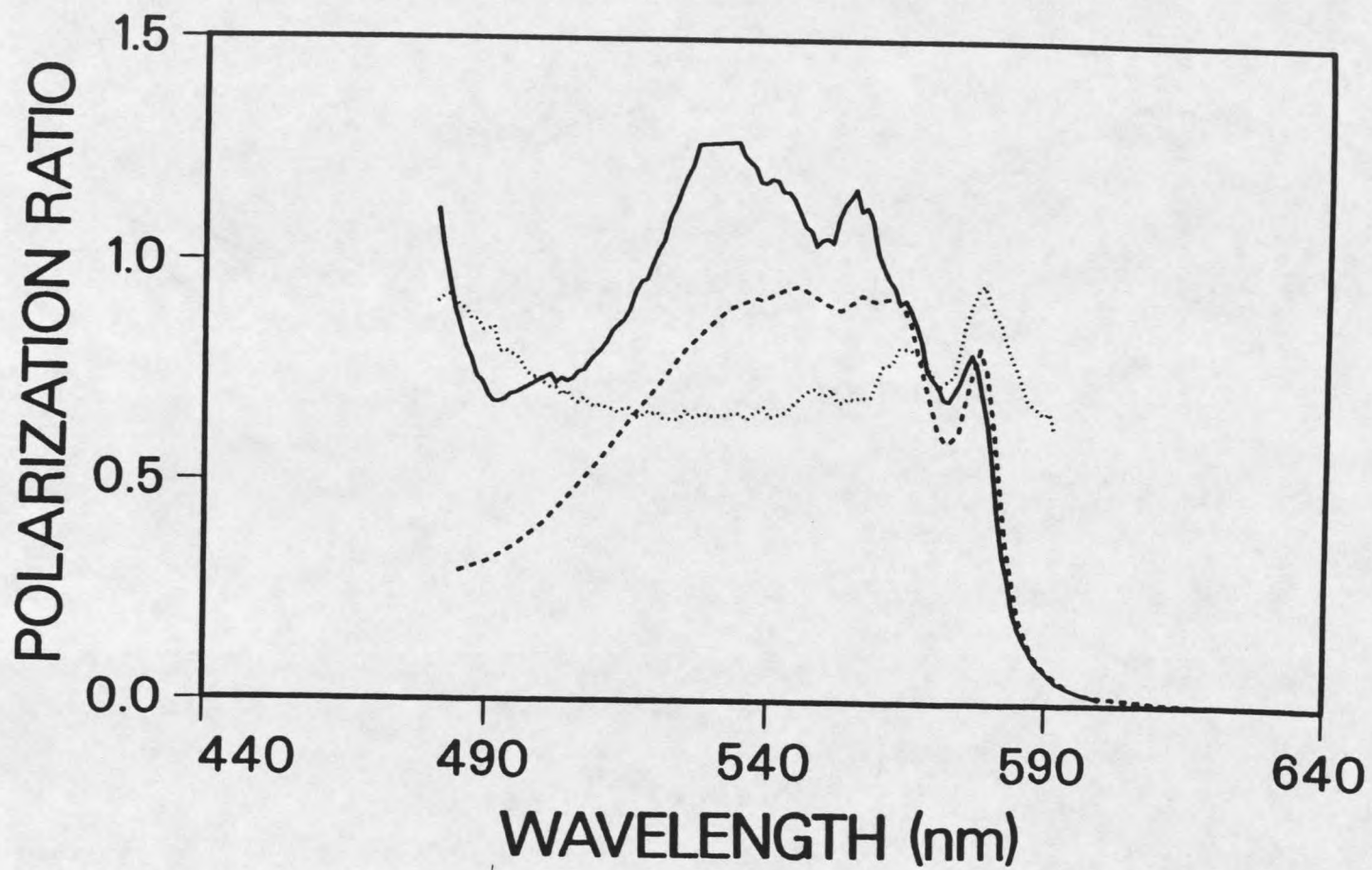


Figure 20: Two-photon fluorescence excitation (solid line), one photon absorption (dashed line), and two-photon polarization (dotted line) spectra for indole dissolved in butanol (0.01M).

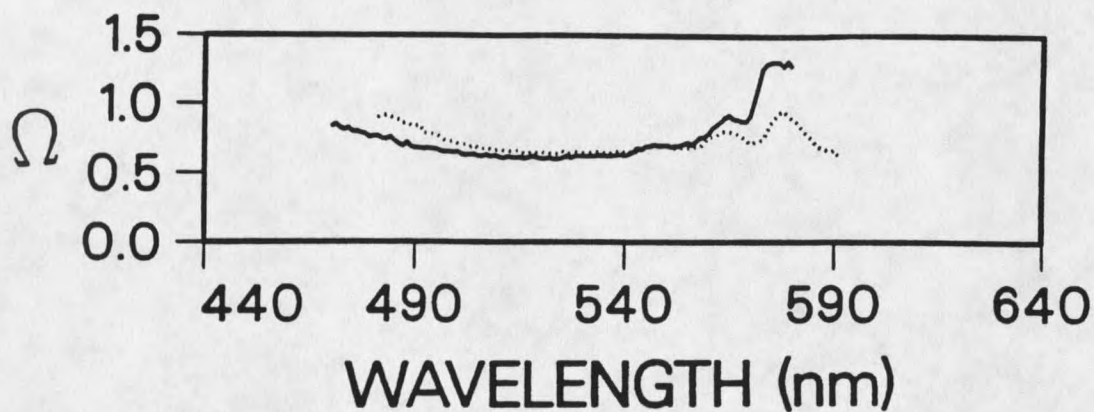


Figure 21: Two-photon polarization spectra of indole in cyclohexane (solid lines) and in butanol (dotted line) (0.01M).

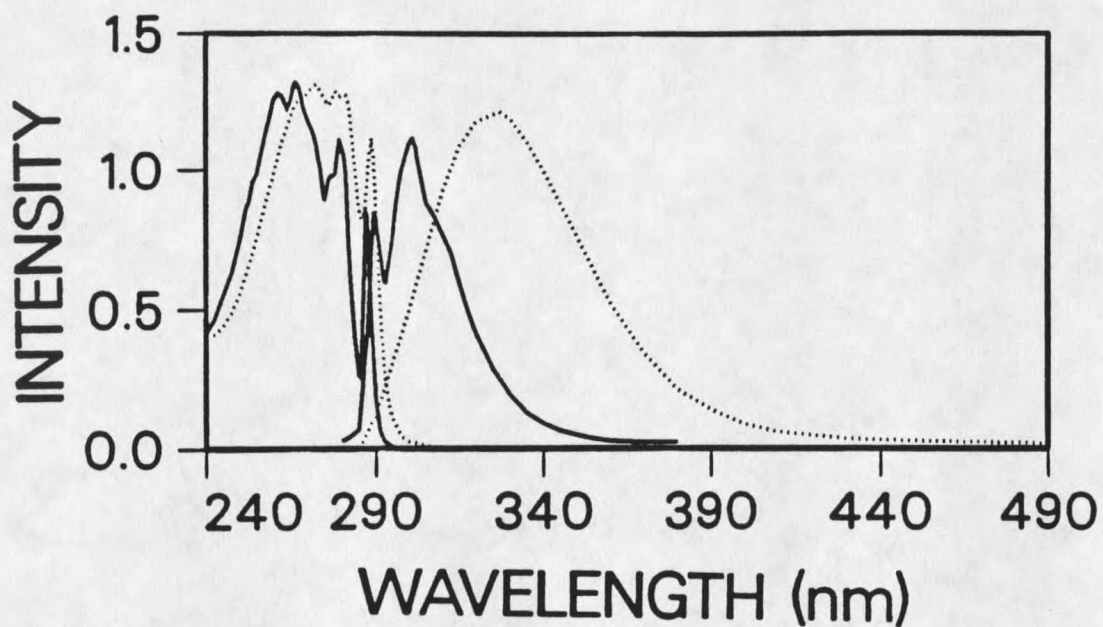


Figure 22: One-photon absorption and fluorescence spectra of indole in cyclohexane (solid lines) and in butanol (dotted line) (0.01M).

1-methylindole. The data for 1-methylindole in butanol (0.01M) are shown in Figs. 23-25. Again the values of  $\Omega$  are lowered in the origin and the fluorescence loses structure and shifts to the red (310 nm to 326 nm).

3-methylindole. The 3-methyl derivative which had the  $L_a$  and  $L_b$  0-0's superposed in cyclohexane now has  $L_a$  as the lowest singlet state. The polarization ratio (Figure 26, 0.01M butanol) at the red edge is about 0.5 as was seen for 2,3 dimethylindole in cyclohexane. The TPA and OPA now appear less steep on the red edge. Figures 27 and 28 show the changes in  $\Omega$  and in the absorption and fluorescence for 3-methylindole.

2,3 dimethylindole. The spectra for 2,3 dimethylindole in butanol (0.01M) are shown in Figure 29 along with the associated changes in  $\Omega$  (Figure 30) and fluorescence (Figure 31). The fluorescence spectra are of interest because they show what fluorescence from  $L_a$  looks like in non-polar and in polar solvents.

4-methoxyindole. This molecule with its reduced  $L_a$  absorption in TPA shows a small drop in  $\Omega$  on the red edge when dissolved in butanol (0.004M) (Figures 32 and 33). The fluorescence maximum shifts from 305 nm to 307 nm (Figure 34) and loses little structure. It appears this molecule emits predominantly from the  $L_b$  state and this is consistent with the high  $\Omega$  value on the red edge.

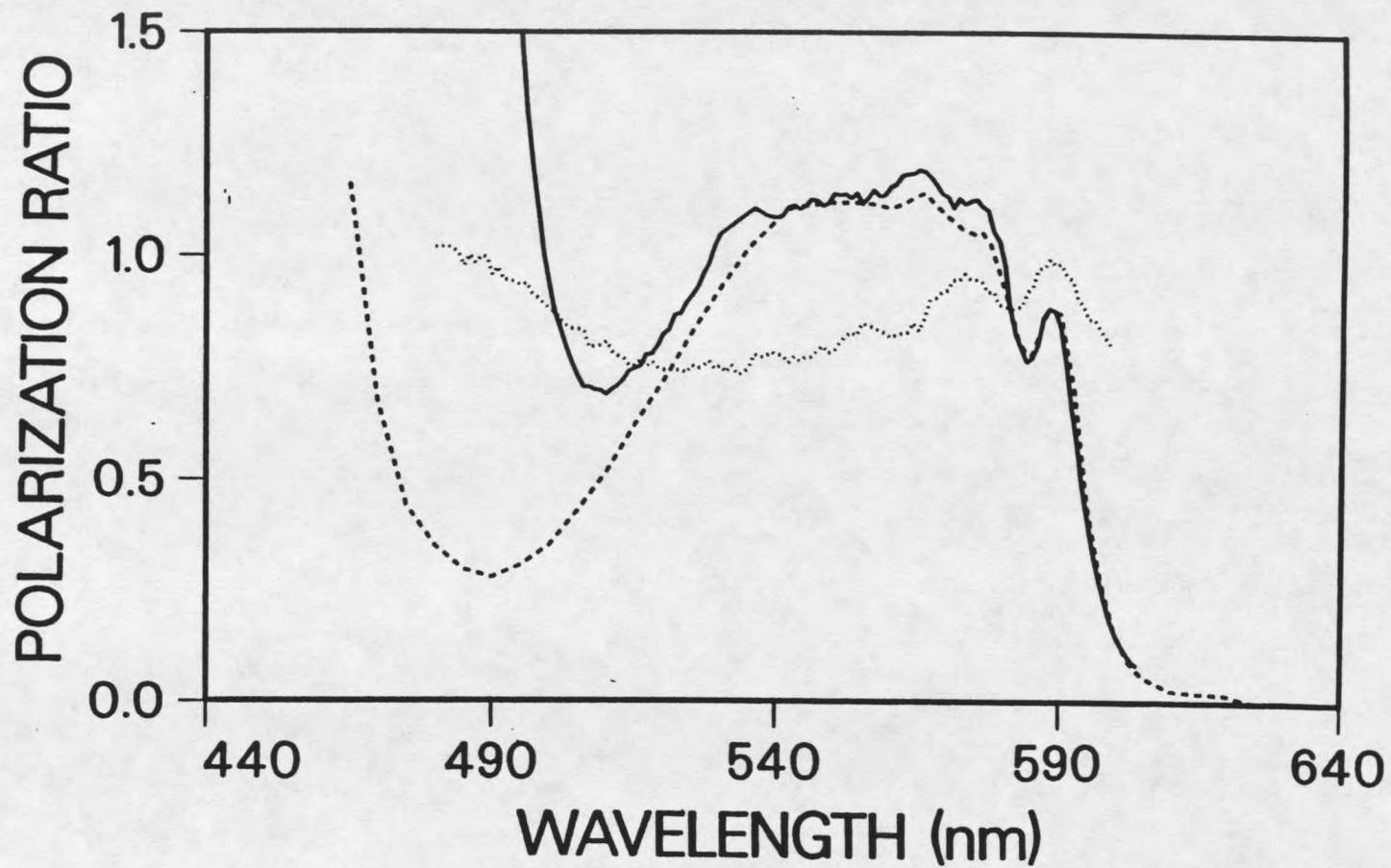


Figure 23: Two-photon fluorescence excitation (solid line), one photon absorption (dashed line), and two-photon polarization (dotted line) spectra for 1-methylindole dissolved in butanol (0.01M).

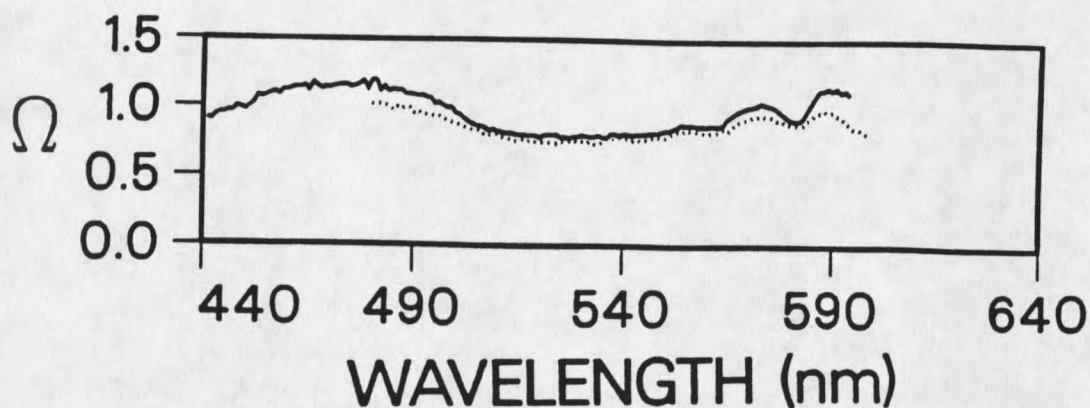


Figure 24: Two-photon polarization spectra of 1-methylindole in cyclohexane (solid line) and in butanol (dotted line) (0.01M)

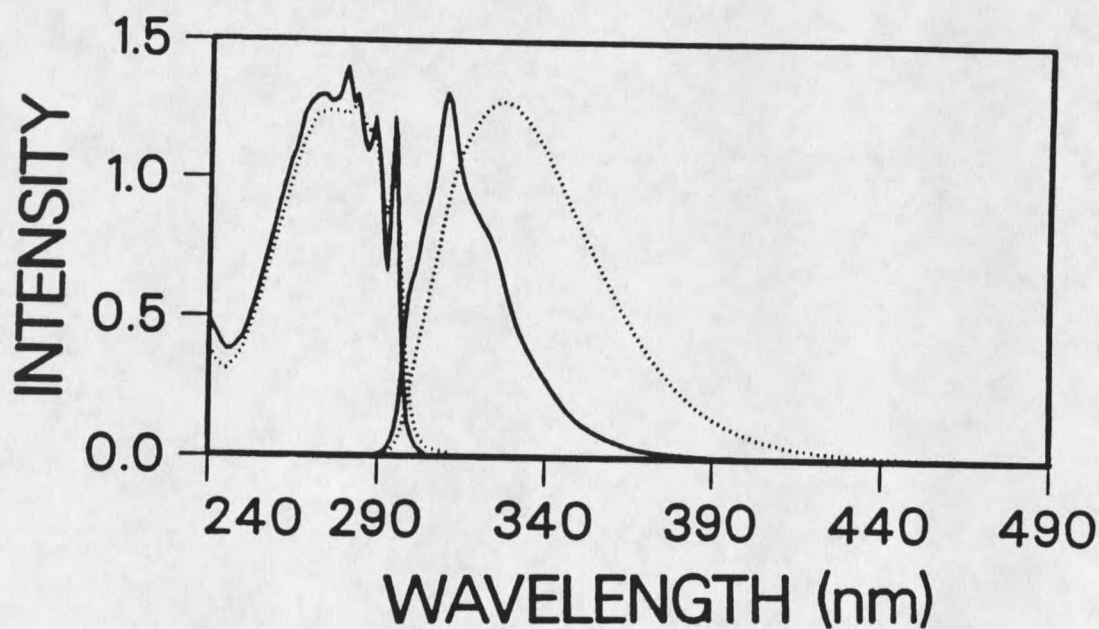


Figure 25: One-photon absorption and fluorescence spectra of 1-methylindole in cyclohexane (solid lines) and in butanol (dotted lines) ( $\sim 10^{-5}$ M).

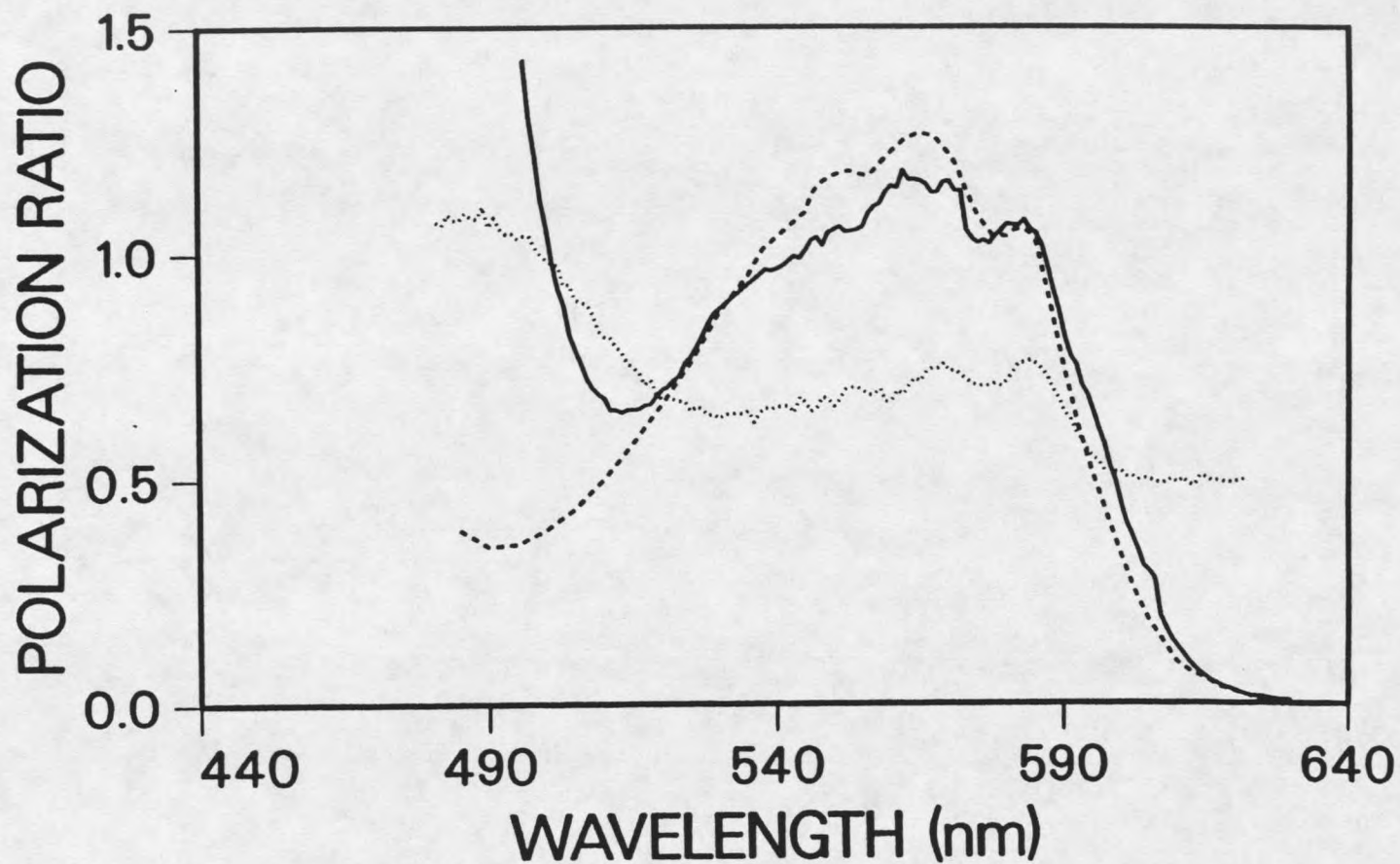


Figure 26: Two-photon fluorescence excitation (solid line), one photon absorption (dashed line), and two-photon polarization (dotted line) spectra for 3-methylindole dissolved in butanol (0.01M).

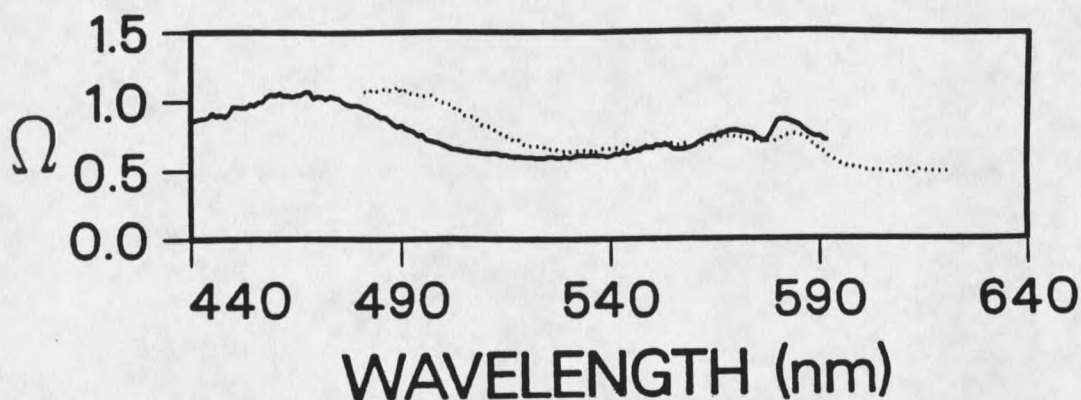


Figure 27: Two-photon polarization spectra of 3-methylindole in cyclohexane (solid line) and in butanol (dotted line) (0.01M).

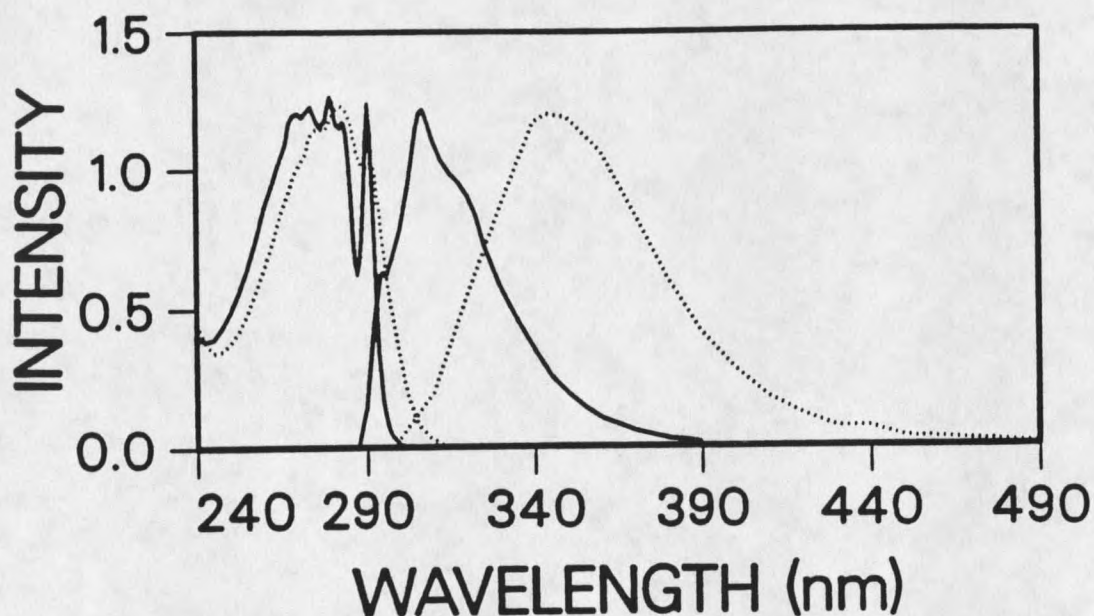


Figure 28: One-photon absorption and fluorescence spectra of 3-methylindole in cyclohexane (solid lines) and in butanol (dotted lines) ( $\sim 10^{-5}$ M).

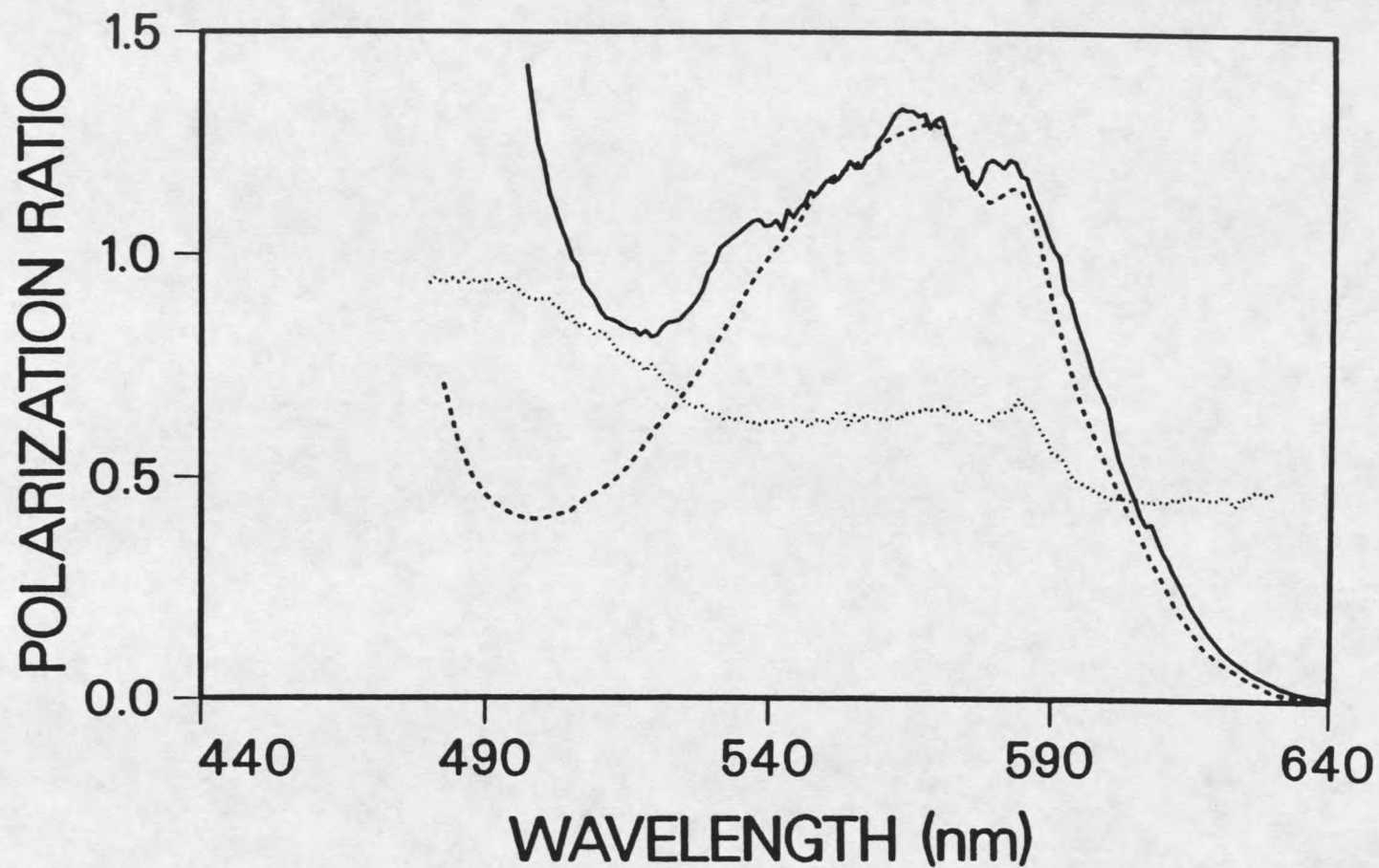


Figure 29: Two-photon fluorescence excitation (solid line), one photon absorption (dashed line), and two-photon polarization (dotted line) spectra for 2,3-dimethylindole dissolved in butanol (0.01M).

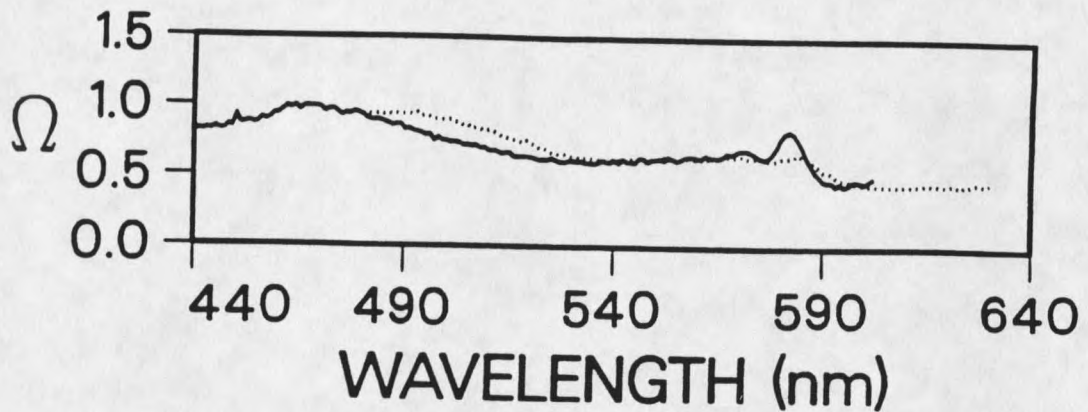


Figure 30: Two-photon polarization spectra of 2,3-dimethylindole in cyclohexane (solid line) and in butanol (dotted line) (0.01M).

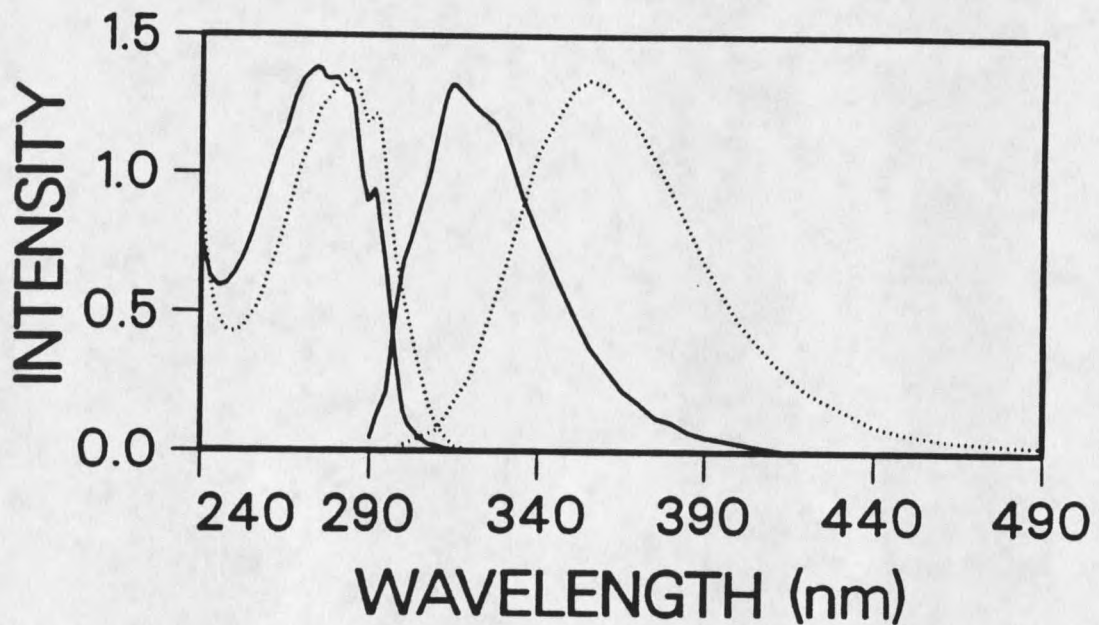


Figure 31: One-photon absorption and fluorescence spectra of 2,3-dimethylindole in cyclohexane (solid lines) and in butanol (dotted lines) ( $\sim 10^{-5}M$ ).

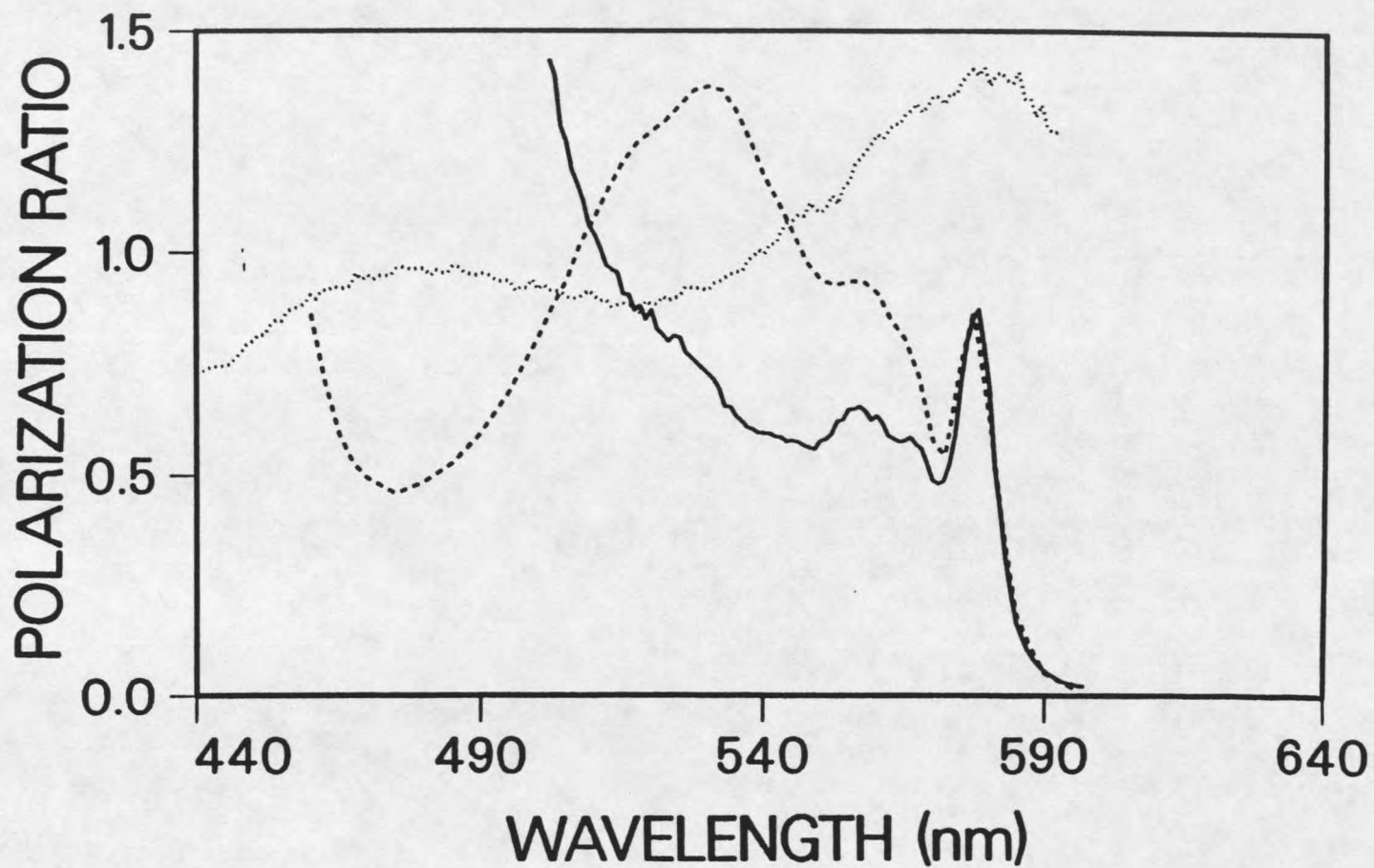


Figure 32: Two-photon fluorescence excitation (solid line), one photon absorption (dashed line), and two-photon polarization (dotted line) spectra for 4-methoxyindole dissolved in butanol (0.004M).

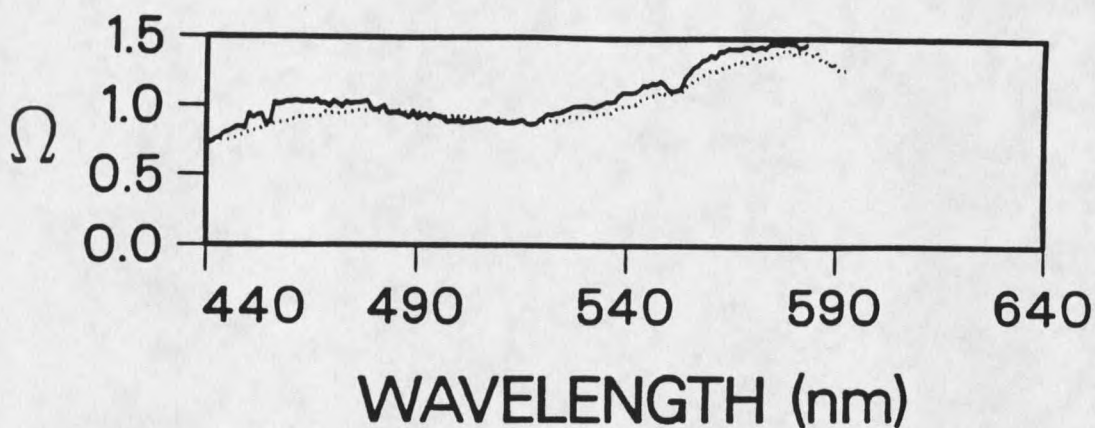


Figure 33: Two-photon polarization spectra of 4-methoxyindole in cyclohexane (solid line) and in butanol (dotted line) (0.004M).

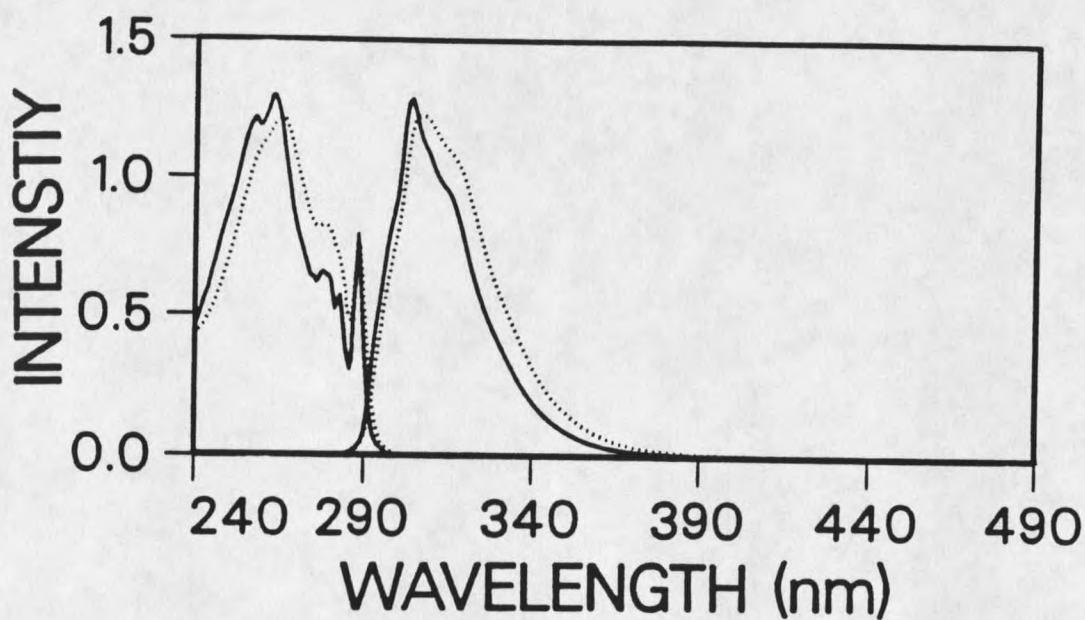


Figure 34: One-photon absorption and fluorescence spectra of 4-methoxyindole in cyclohexane (solid lines) and in butanol (dotted lines) ( $\sim 10^{-5}M$ ).

5-methoxyindole. The broad  $L_a$  state shifts red and covers most of the  $L_b$  state for 5-methoxyindole in butanol (0.004M) (Figure 35). The  $\Omega$  value on the red edge never changes and correspondingly there is only a shift in fluorescence maximum from 327 nm to 330 nm with very little broadening (Figures 36 and 37), indicating  $L_b$  fluorescence.

6-methoxyindole. The TPA shows very little  $L_a$  intensity (Figure 38) for this molecule (0.004M butanol) and the peak not seen in OPA is also evident in butanol solvent.  $\Omega$  drops on the red edge and the fluorescence maximum shifts from 318 nm to 334 nm and becomes much broader (Figures 39 and 40). 6-methoxyindole is the only methoxyindole which shows such a large red shift. Perhaps the  $L_b$  state is more sensitive to solvation when it is substituted at position 6.

7-methoxyindole. As the broad  $L_a$  shifts red in the polar solvent, the  $\Omega$  value at the origin drops and the 2 peaks associated with the  $L_b$  band are somewhat smeared out (Figure 41, 0.004M butanol). However, virtually no change in fluorescence is observed, the maximum staying at 305 nm. (Figures 42,43). It is likely that this molecule emits from  $L_b$ .

### Discussion

Assigning a high polarization ratio of  $\sim 1.4$  to the  ${}^1L_b$  state and a low ratio of  $\sim 0.5$  to the  ${}^1L_a$  state gives a general picture in accord with that deduced from one-photon

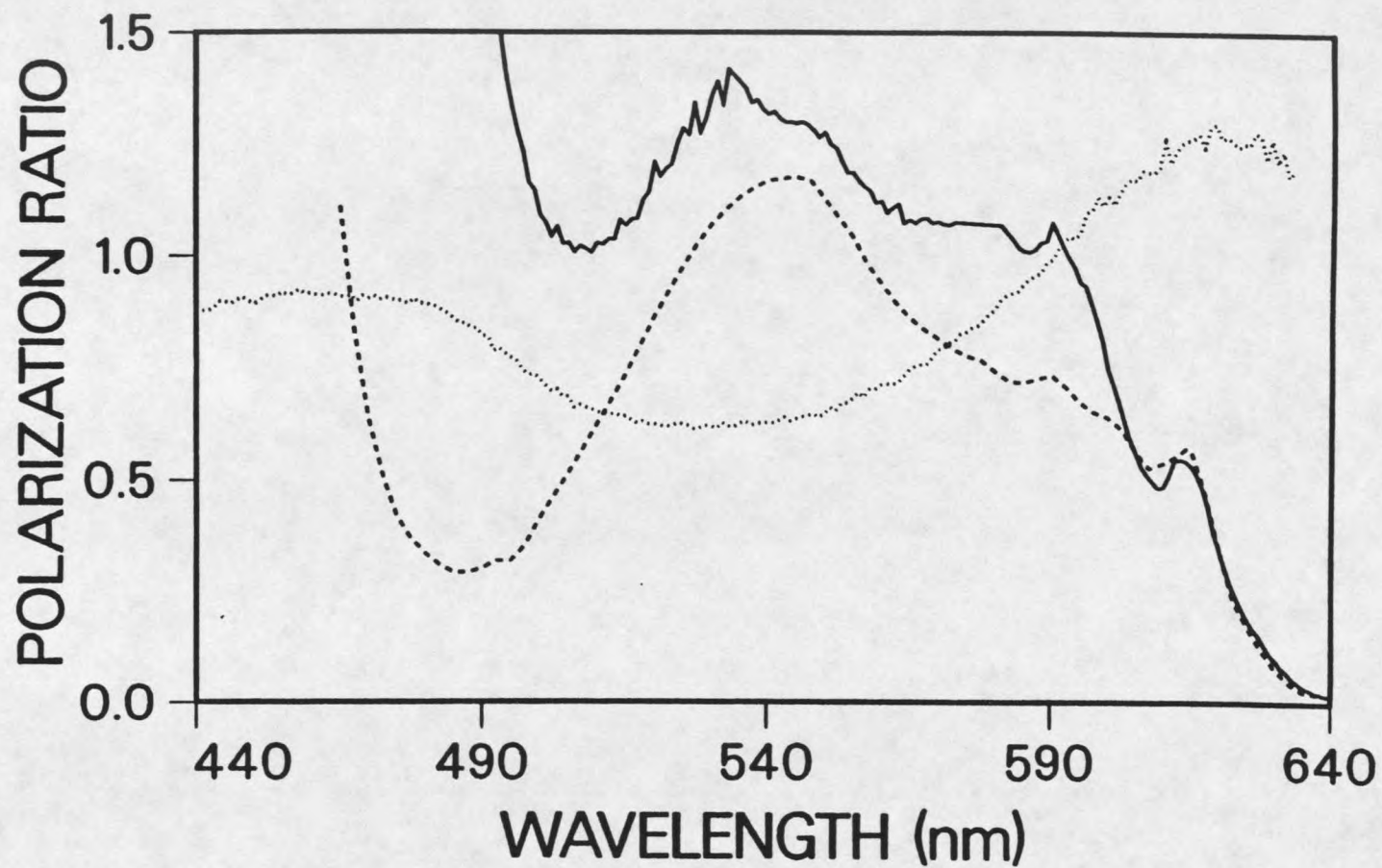


Figure 35: Two-photon fluorescence excitation (solid line), one photon absorption (dashed line), and two-photon polarization (dotted line) spectra for 5-methoxyindole dissolved in butanol (0.004M).

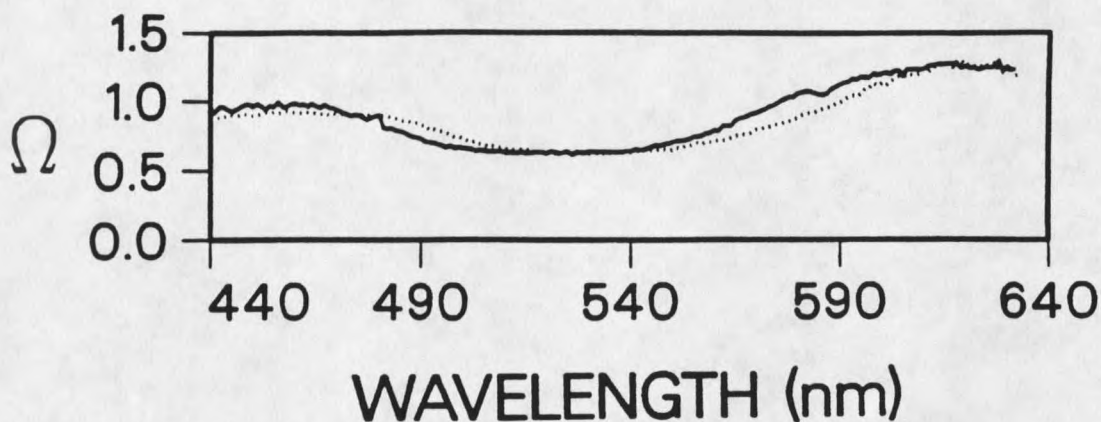


Figure 36: Two-photon polarization spectra of 5-methoxyindole in cyclohexane (solid line) and in butanol (dotted line) (0.004M).

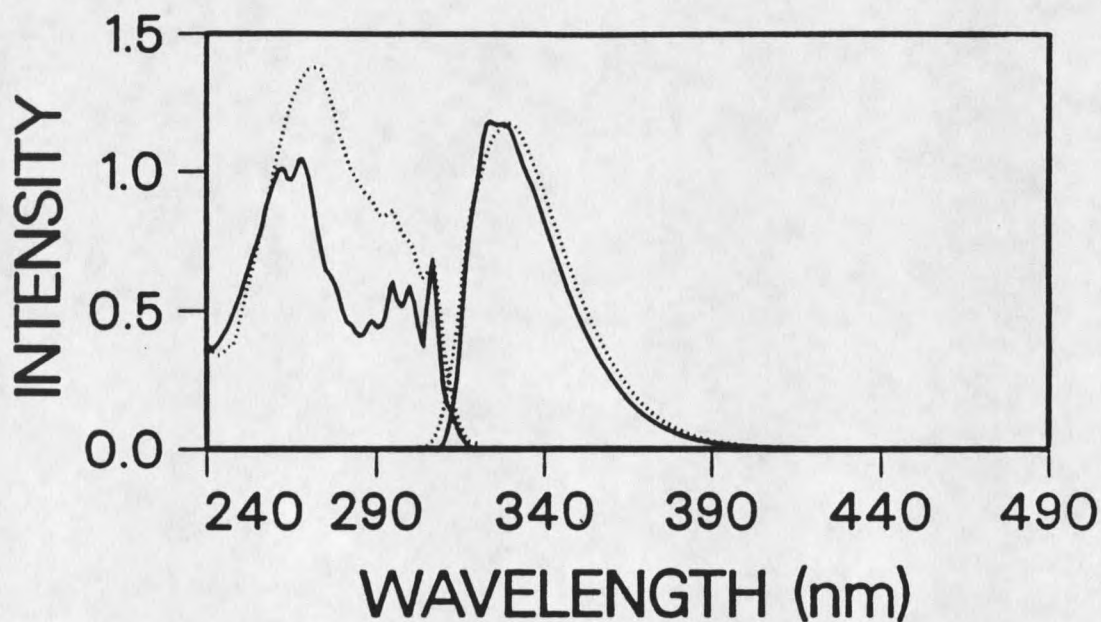


Figure 37: One-photon absorption and fluorescence spectra of 5-methoxyindole in cyclohexane (solid lines) and in butanol (dotted lines) ( $\sim 10^{-5}$ M).

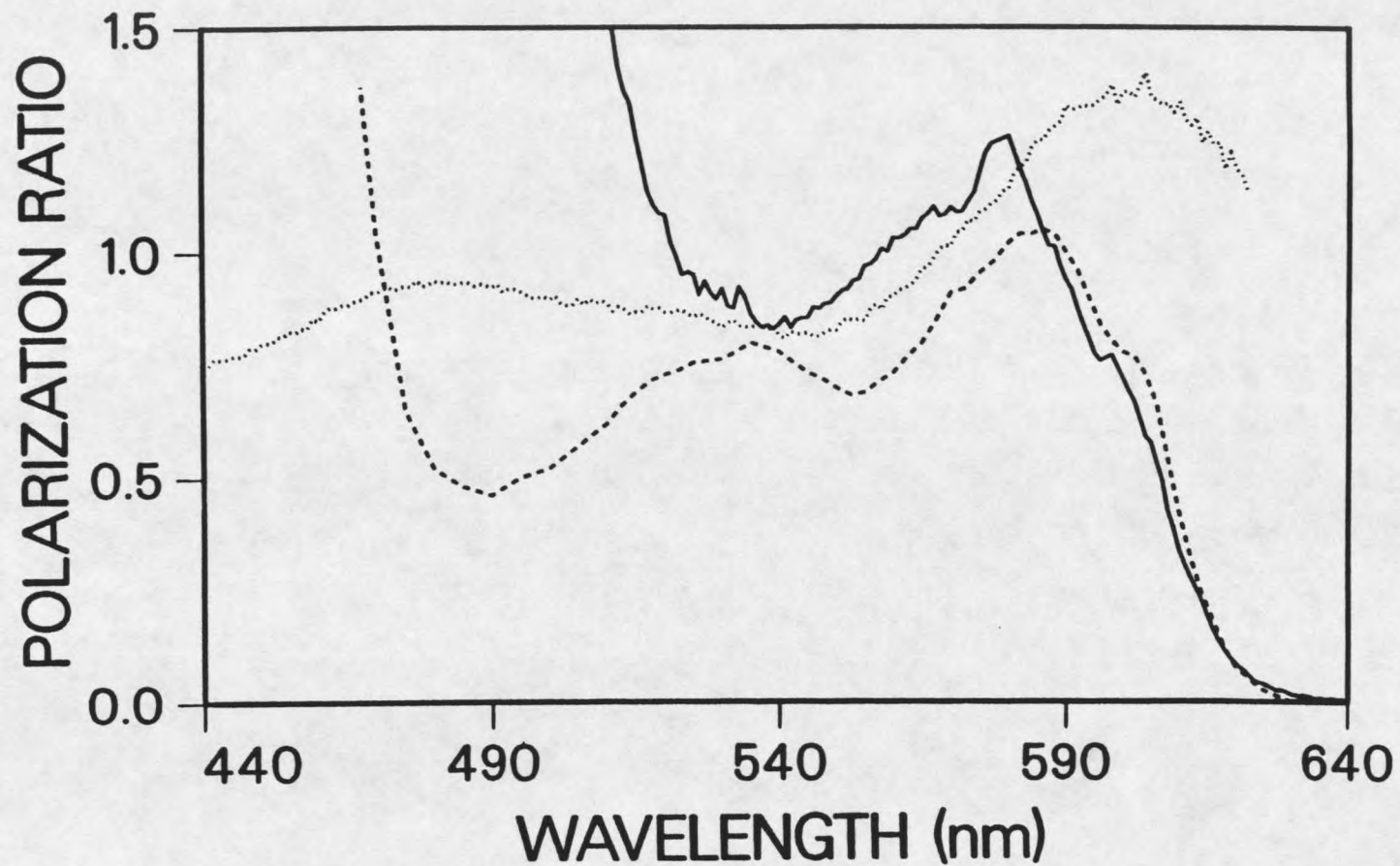


Figure 38: Two-photon fluorescence excitation (solid line), one photon absorption (dashed line), and two-photon polarization (dotted line) spectra for 6-methoxyindole dissolved in butanol (0.004M).





























































































